NASA TECHNICAL NOTE

A STUDY OF SEVERAL OXIDATION-RESISTANT COATINGS ON Cb-10Ti-5Zr ALLOY SHEET AT 2000° F, 2400° F, AND 2700° F (1365° K, 1590° K, AND 1755° K)

by W. Barry Lisagor and Bland A. Stein

Langley Research Center
Langley Station, Hampton, Va.

NATIONAL AERONAUTICS AND SPACE ADMINISTRATION • WASHINGTON, D. C. • MARCH 1966

NASA TN D-3213

A STUDY OF SEVERAL OXIDATION-RESISTANT COATINGS

ON Cb-10Ti-5Zr ALLOY SHEET AT 2000° F, 2400° F,

AND 2700° F (1365° K, 1590° K, AND 1755° K)

By W. Barry Lisagor and Bland A. Stein

Langley Research Center
Langley Station, Hampton, Va.

NATIONAL AERONAUTICS AND SPACE ADMINISTRATION

A STUDY OF SEVERAL OXIDATION-RESISTANT COATINGS

ON Cb-10Ti-5Zr ALLOY SHEET AT 2000° F, 2400° F,

AND 2700° F (1365° K, 1590° K, AND 1755° K)

By W. Barry Lisagor and Bland A. Stein
Langley Research Center

SUMMARY

Results of a study on the properties of Cb-10Ti-5Zr columbium alloy sheet with 12 oxidation-resistant coatings are presented. Oxidation tests were performed in dry air at 2000° F, 2400° F, and 2700° F (1365° K, 1590° K, and 1755° K) at atmospheric pressure and also at pressures of 0.5 and 0.05 torr $(67$ and 6.7 $N/m^2)$. Mechanical-property tests included room-temperature and elevated-temperature tensile tests on both uncoated and coated material before and after exposure and room-temperature bend tests on oxidation coupons before and after exposure. Test results indicate that an upper limit for protection of this alloy from oxidation is approximately 2400° F (1590° K) using modified silicide coatings containing titanium and chromium and that the usefulness of thin-gage coated columbium alloy sheet may be determined by substrate embrittlement rather than by oxidation.

Comprehensive metallurgical examinations on as-coated and tested specimens were performed by using X-ray emission and diffraction techniques and electron-probe micro-analyzer studies. Substrate thickness decreases due to solid-state diffusion during high-temperature exposures were determined. A possible embrittling mechanism for the coated Cb-10Ti-5Zr alloy sheet is postulated and supported by the metallurgical studies.

INTRODUCTION

When aerospace vehicles experience conditions associated with reentry or hypersonic flight, they are subjected to high temperatures for various intervals of time. Metallic shields, which dissipate aerodynamic heating by radiation, have been used to protect thermally certain areas of these vehicles. Columbium is a candidate material for the construction of these heat shields because of its high-temperature mechanical properties and its relatively low density compared with other refractory metals. The development of several columbium alloys has progressed rapidly, and has led to many

evaluations of physical properties (for instance, refs. 1 and 2), joining techniques (refs. 3 and 4), and structural design and manufacturing methods (ref. 5). The fabrication and testing of actual heat-shield designs for coated molybdenum and uncoated columbium alloys have also been investigated. (See, for example, ref. 6.)

Columbium experiences rapid oxidation when subjected to oxidizing environments at elevated temperatures. The reaction product is primarily Cb_2O_5, a nonprotective porous oxide with no load-carrying capability. For this reason columbium alloys must be coated with a continuous, adherent coating which will provide protection against oxidation and will also provide a barrier to the diffusion of contaminating gases which could have adverse effects on the mechanical properties of the substrate material. The coating itself must have as little effect as possible on the substrate mechanical properties. There have been several evaluations (refs. 7 and 8, for example) on some coating systems for various columbium alloys. These evaluations indicate that the greatest problem is the lack of consistent results in oxidation tests. However, there are coating systems which have shown promise for possible use and reuse in the thermal protection systems of aerospace vehicles.

The program described herein was initiated to determine the present status of oxidation-resistant coatings for columbium alloy sheet. Mechanical properties of Cb-10Ti-5Zr columbium alloy sheet with 12 oxidation-resistant coatings were evaluated in air under various conditions of temperature and pressure. Emphasis was directed towards categorizing the constituents of promising coatings and investigating the phenomena involved in coating failure and substrate embrittlement. The units used for the physical quantities in this paper are given both in the U.S. Customary Units and in the International System of Units (SI) (ref. 9). The conversion factors required for units used in the present study are presented in appendix A.

SPECIMENS

Materials

The specimens utilized in this investigation were fabricated from Cb-10Ti-5Zr columbium alloy sheet, with a nominal thickness of 0.020 inch (0.50 mm). The material was procured from a commercial supplier in the annealed condition and fabricated into test specimens. Specimens included small oxidation coupons $\frac{3}{4}$ by $1\frac{1}{2}$ inches (1.9 by 3.8 cm) and tensile strips $4\frac{1}{8}$ by $\frac{5}{8}$ inches (10.5 by 1.6 cm) with a 2-inch (5.1 cm) gage length reduced to 3/8 inch (0.95 cm). After the specimens were machined to size, they were tumbled in a small laboratory tumbling mill approximately 24 hours, with dry 180 mesh silicon carbide abrasive, until the edges of the specimens were rounded to a smooth radius. Specimens were cleaned in acetone after tumbling. The mass and

average thickness was then determined for each specimen before it was sent to the coating vendors.

Coatings

Nine coating vendors participated in the investigation, three vendors supplying two coatings each for a total of 12 coatings. Coating vendors were requested to supply a coating which would provide maximum oxidation resistance at temperatures from 1500° F to 3000° F (1090° K to 1920° K) with no more than a 25-percent change in mechanical properties with respect to the uncoated material. Coating identification and methods of application are listed in table I.

TEST PROCEDURES

X-ray and Metallurgical Examination

Specimens were measured for thickness and mass changes upon receipt from the coating suppliers, and a thorough X-ray examination of the specimen surface was conducted for a typical specimen of each coating. The X-ray analysis consisted of both diffraction and emission examinations in an attempt to identify both compounds and elements. The specimens which were utilized in the X-ray study were then mounted on edge in a 1-inch (2.5 cm) diameter metallurgical mount and ground with 120, 240, 400, and 600 grit wet emery in successive steps. Polishing was accomplished by using 5-micron (5 μm) alumina on silk and 0.3-micron (0.3 μm) alumina on microcloth. Etch-polish-etch techniques were employed, an etchant composed of 30 parts lactic acid, 10 parts nitric acid, and 10 parts hydrofluoric acid being used. Specimens were then examined metallographically, and coating thicknesses were measured by using a metallurgical microscope with a calibrated filar micrometer eyepiece. The coating thicknesses represent an average of at least 10 readings on each coating and are listed in table I. Some of the coatings appear cracked in the photomicrographs and this cracking was caused primarily by metallurgical preparation after testing and should not be construed as test damage.

Mechanical Property Tests

Room-temperature mechanical property tests consisted of tensile tests and bend tests. The tensile stress-strain tests were conducted in both mechanical and screw-driven testing machines. Strain was measured with optical strain gages or microformer-type extensometers. Elongation was measured in a 1-inch (2.54 cm) gage length. Room-temperature tensile tests were conducted on specimens of each coating as coated and after 1-hour and 8-hour exposures in laboratory air at 2400° F (1590° K). Tests were

also made on uncoated material exposed in a vacuum of 10^{-5} torr (1.33 N/m^2) at 2400° F for the same lengths of time.

Elevated-temperature tensile tests were conducted on the uncoated alloy and on specimens of each of the 12 coatings at 2000° F and 2400° F (1365° K and 1590° K). Specimens were resistance heated to temperature and held for 6 minutes before testing. The uncoated material was tested in argon of 99.96-percent minimum purity with a dewpoint of -90° F (205° K) whereas coated specimens were tested in air. All elevated-temperature tests were made in a screw-powered machine. Temperatures were monitored with a platinum—platinum-13-percent-rhodium thermocouple for the uncoated material and by an optical pyrometer for the coated specimens. The observed temperatures for the coated specimens were corrected by using an assumed emittance value of 0.8.

Room-temperature bend tests were made on oxidation tabs as coated and after exposure in air at 2000° F, 2400° F, and 2700° F (1365° K, 1590° K, and 1755° K) to evaluate further the ductility in the specimens after exposure. The tests were conducted by using a mechanical screw power machine in conjunction with the apparatus described in reference 10. Loading span was nominally 1 inch (2.54 cm) with a nominal ram bend radius of 1/16 inch (0.16 cm). Specimens were limited to a center-point deflection of 0.5 inch (1.3 cm) which resulted in a bend angle of approximately 90°.

Oxidation Tests

Oxidation tests were conducted on all coatings at 2000° F, 2400° F, and 2700° F (1365° K, 1590° K, and 1755° K) at atmospheric (101 kN/m^2) pressure. Specimens were exposed to dry air, with a dewpoint of approximately -40° F (233° K), at a flow rate of 1.5 standard cubic feet per hour $(12 \text{ cm}^3/\text{s})$ both continuously and cyclically. During the continuous tests, specimens were weighed by using a thermogravimetric balance described in reference 11. After a 10-percent weight gain or 240-hour exposure, testing was discontinued and specimens were examined visually to determine the extent of the damage and then bend tested, if possible.

Cyclic oxidation tests consisted of 1-hour exposures in dry air at 2000° F, 2400° F, and 2700° F. Specimens were placed in zirconium silicate boats and suspended in vertical tube furnaces using platinum wire. The furnaces were stabilized at the test temperature prior to insertion of the specimens. When the specimens were placed in the furnace, they rapidly attained the test temperature. After each cycle specimens were allowed to air cool and were weighed before the next cycle. Tests were terminated when visual damage was evident or after 240 cycles, and then bend tested. Cyclic oxidation tests were also performed on four coatings at 2400° F (1590° K) and at air pressures of 0.5 torr (67 N/m^2) and 0.05 torr (6.7 N/m^2). Specimens were weighed after each

1-hour cycle. Gas flow rates were very low because of the low capacity pumping system which was utilized in this phase of the investigation.

Diffusion tests.- Coupon specimens of several coatings were exposed in both argon and laboratory air at temperatures ranging from 2400° F (1590° K) to 2700° F (1755° K) to determine substrate recession rate. After each exposure specimens were sectioned and examined metallographically, a filar micrometer eyepiece being used, to determine the reduction in substrate thickness.

Electron microprobe analysis.- An electron probe X-ray microanalyzer was utilized to examine some specimens in the as-received condition and after high-temperature exposure to determine, if possible, the mechanisms which cause changes in mechanical properties or which affect the oxidation process itself. Sample current, back-scattered electrons, and X-ray emissions of the various elements were monitored on both oscilloscopes and recorder charts. Uncoated Cb-10Ti-5Zr alloy was used for a standard Zr concentration of 5 percent.

RESULTS AND DISCUSSION

In evaluating the results of this investigation, no effort was made to rate coatings on the basis of the relatively small number of tests performed for each coating. Efforts were made to identify the compounds and additive elements present in the coatings which provided adequate oxidation resistance with least substrate embrittlement in the tests. This section, in describing the results of the present investigation will first consider each coating separately in terms of coating composition and performance of specimens in the various mechanical property and oxidation tests. Specific coatings will be discussed and general comments concerning the behavior of the coatings that were found to provide the best oxidation resistance for the Cb-10Ti-5Zr columbium alloy will be made. Since the results indicated that substrate embrittlement appears to be a limiting factor for the high-temperature operation of coated thin-gage columbium alloys in structural applications, considerable efforts were directed toward identifying the embrittling mechanisms for several of the coatings and one such mechanism is postulated herein.

X-ray analysis data for all coatings are given in table II. Room-temperature tensile data are given in table III and figure 1, and elevated temperature tensile data are given in table IV. Results of the bend tests conducted on the oxidation coupons are given in table V.

It should be noted that the X-ray results in table II are only semiquantitative in nature. Results for each element can be compared for different coatings to show concentration trends of the given element but comparisons of relative concentrations of different

elements in one coating cannot be made; that is, Cb intensity can be compared in all 12 coatings, but Cb intensity cannot be compared or correlated with Si intensity for a single coating.

Specific Coatings

Coating 1.- A relatively high columbium intensity was noted in the X-ray emission examination of the surface of coating 1. Also identified were Ti, Cr, Zr, Fe, and Si. The Fe intensity was high whereas the Si intensity was low. X-ray diffraction analysis indicated the primary compound to be CbB_2. It should be noted here that boron is presently unidentifiable by X-ray emission techniques because the low-energy characteristic X-rays of boron cannot be detected. The as-received appearance of specimens of coating 1 is shown in figure 2. Substrate appearance may be compared with cross sections of the uncoated columbium alloy sheet in figure 3. The coated surface was dull black in color and relatively smooth in texture, some signs of nonuniformity being indicated by areas of different texture. Comparison of the uncoated grain size (fig. 3) and the substrate grain size in the coated specimen (fig. 2) indicates that some substrate grain growth resulted from the coating procedure. The metallographic studies showed some indications of substrate contamination due to the coating operation as evidenced by the appearance of precipitate particles. However, no indication of a continuous network of contaminants was observed in the substrate.

The results of the room-temperature tensile tests (table III) indicated that the coating procedure reduced the tensile elongation from 30 to 14 percent. The data for the uncoated specimens are in good agreement with the data presented in reference 2. Elevated-temperature test results (table IV) show a slight increase in ultimate tensile strength for specimens of coating 1 compared with the uncoated material. The low elongation value for the uncoated material at 2400° F (1590° K) in table IV may be due in part to a localized hot spot in the failure zone, caused by resistance heating of the specimens. Initial necking down in the failure zone causes a smaller current path and the temperature increases rapidly with further plastic deformation. There was no evidence of a surface reaction and the surfaces were very clean after the test in argon of the reported purity. On coated specimens, the existence of the coating appeared to reduce this necking-down hot-spot effect.

The results of the continuous and cyclic oxidation tests at 2000° F, 2400° F, and 2700° F (1365° K, 1590° K, and 1755° K) are shown in figure 4. In presenting oxidation data for this coating and each of the subsequent coatings, plots of mass change as a logarithmic function of time are given. In general, initial oxidation damage during continuous testing is observed as an increasing rate of mass gain, and during cyclic testing, as a mass loss because of coating and oxide spall-off. As previously mentioned, the time at

6

which these rate changes occur was taken as the time of coating failure. For coatings which provide good oxidation protection for the substrate, these points are easily noted as will be seen in subsequent figures. For coating 1, general specimen appearance after exposure was different in color and texture for each of the temperatures investigated as can be seen in figure 5. This behavior indicates that the reaction products may differ in composition for each temperature investigated. The failure at 2000° F (1365° K) appeared to be due to coating failure and oxidation of the substrate whereas failure at 2700° F (1755° K) actually appears to be caused by melting of the reaction products after formation of low melting compositions by solid-state diffusion. All specimens failed very rapidly at 2700° F (1755° K).

Coating 2.- Results of the X-ray analysis (table II) showed the same elements present as for coating 1 and again the primary phase identification by X-ray diffraction was CbB_2. Coating appearance in the as-received condition is shown in figure 6. The surface appearance of the coating was similar to that of coating 1, but the coating thickness was approximately twice that of coating 1 (table I). Metallographic examination of coating 2 showed that the substrate itself was more severely affected by contaminants; as a result there was a continuous network of precipitates in the grain boundaries and subsequent severe embrittlement. The room-temperature tensile test results are shown in table III. The marked change in tensile properties indicate severe alteration of the base material by the coating process itself. The process lowered the tensile strength from 76 ksi to 49 ksi $\left(525 \text{ to } 338 \text{ MN/m}^2\right)$ increased the elastic modulus from 15×10^6 to 24×10^6 psi $\left(103 \text{ to } 166 \text{ GN/m}^2\right)$ and completely embrittled the substrate. Results of the elevated-temperature tensile tests (table IV) indicate the resultant specimen is actually stronger at 2400° F than the uncoated material, but tensile elongation was still negligible at 2000° F (1365° K) and only 4 percent at 2400° F (1590° K). Results of the bend tests also indicated complete embrittlement of substrate as found in the tensile tests (table I).

Results of the cyclic and continuous oxidation tests are shown in figure 7, and the appearances of exposed specimens are shown in figure 8. Again, as was noted in coating 1, specimen appearance after exposure suggested different reaction products at all three test temperatures. Failure at 2700° F (1755° K) occurred immediately on insertion into the furnace and appeared to be caused by melting of the specimen rather than by oxidation of the substrate.

Coating 3.- Although the coating procedure consisted of a first cycle of silicon and a second cycle of chromium and boron, the primary outer structure was found to be $CbSi_2$ and Cb_5Si_3 (table II). The appearance of this coating in the as-received condition is shown in figure 9. The coating appearance was dull gray, relatively smooth in texture, but had some darker spots dispersed over the entire coating. Once again, grain growth

in the substrate occurred during the coating procedure. Metallographic studies indicated only very slight pickup of precipitates in the substrate.

Room-temperature tensile test results (table III) indicate that the coating process reduced the tensile elongation of the substrate from 30 percent to 19 percent. However, after 1-hour exposure in air at 2400° F (1590° K), the substrate was embrittled and exhibited negligible elongation with no appreciable effect on tensile strength or elastic modulus. The low ultimate strength after the 8-hour exposure may be due, in part, to oxidation damage. High-temperature tensile test results indicated no significant change in tensile strength compared with the uncoated material. Results of the bend ductility tests on coating 3 indicated no serious loss of bend ductility (table IV).

Oxidation test results are shown in figure 10, and appearance of exposed specimens is shown in figure 11. Cyclic exposure reduced coating life as can be seen in figure 10. All observed failures on the cyclically exposed coupons of this coating initiated on the specimen edges. There was no visual evidence of glass formation at 2000° F (1365° K) and 2400° F (1590° K) but specimens exposed at 2700° F (1755° K) exhibited a visible glassy surface. Failure at 2700° F occurred in less than 3 hours for all specimens tested with this coating. There appeared to be different mechanisms of failure for different test temperatures. At 2000° F and 2400° F there was evidence of Cb_2O_5 on the failed specimens. At 2700° F, however, there was no evidence of oxide formation, but some areas appeared to have melted. These melted areas could be caused by the formation of Cb_2O_5 and subsequent melting of this oxide which appeared to flux the coating and/or substrate.

Coating 4.- Results of the X-ray study on coating 4 (table II) indicated a relatively high columbium and silicon content on the surface of the coating. Also identified in the coating were titanium and zirconium from the substrate and chromium and cobalt from the coating operation. The primary crystal structure was identified by X-ray diffraction as $CbSi_2$. Appearance of this coating in the as-received condition is shown in figure 12. The coating appearance was light gray, relatively smooth, and uniform in texture. Cross-sectional views of this coating show no apparent change in the substrate grain size, compared with the uncoated material (fig. 3), and indicated a relatively low temperature coating operation. No gross substrate impurity pickup was apparent from the coating process. The application of coating 4 had little effect on ultimate and yield strength and elastic modulus but tensile elongation was reduced from 30 percent to 20 percent (table III). Exposures in air at 2400° F (1590° K) for 1 and 8 hours reduced the elongation to 12 and 16 percent, respectively. Elevated-temperature tensile test results (table IV) show a small increase in ultimate tensile strength but tensile elongation increased to 19 and 38 percent at 2000° F and 2400° F, respectively, and indicated no embrittling effect in the substrate at these temperatures for short times. Results of

the bend ductility tests indicate that after severe oxidation damage, specimens become embrittled (table V).

Results of the oxidation tests at atmospheric pressure and reduced pressures are shown in figure 13, and the appearance of exposed specimens is shown in figure 14. There was little oxidation damage before 100 hours at 2000° F and the effect of cycling was very small. At 2400° F (1590° K) there was little damage for 30 hours in any of the continuous tests. At 2700° F (1755° K) continuously tested specimens were tested 40 hours before evidence of damage. However, during cyclic testing, one specimen failed after 9 hours and another failed on the first cycle.

After 29 and 54 hours of cyclic exposure at 2400° F (1590° K) there was little or no loss in bend ductility (table V). These specimens were not appreciably damaged by oxidation. Other specimens with visible oxidation damage did become embrittled.

Low pressure oxidation tests were conducted on coating 4, and the results for 2400° F (1590° K) tests at 0.5 and 0.05 torr $\left(67 \text{ and } 6.7 \text{ N/m}^2\right)$ are presented also in figure 13 and photographs of exposed specimens are shown in figure 15. Small mass gains were noted after 20 hours of cyclic testing. Bend tests on these specimens (table V) indicated no loss in bend ductility for this coating. These results indicate no serious coating damage at the pressures tested for very low mass flow rates of laboratory air.

Coating 5.- Coating 5 was produced in exactly the same manner as coating 4 with an additional silicon carbide overcoat applied on one side of the specimens. The purpose of this overcoat was to provide a high emittance surface for maximum radiation of thermal energy. This SiC overcoat was identified by X-ray diffraction (table II), but was not investigated further in this program. The coating appearance is shown in figure 16. The overcoated side has a smooth green texture, and is relatively uniform in appearance. The cross-sectional views look similar to those of coating 4 except that the silicon carbide layer is easily visible. There was essentially no difference in the tensile properties (tables III and IV) or in the bend properties (table V) between coatings 4 and 5. Oxidation test results at atmospheric pressure and the appearance of exposed specimens are shown in figures 17 and 18, respectively.

Coating 6.- Results of the X-ray study on coating 6 (table II) indicate a relatively low silicon and columbium intensity, high chromium intensity, and appreciable intensity of titanium and chromium. X-ray diffraction and emission comparisons indicate the primary compound to be a solid solution of $CbSi_2$ and $CrSi_2$. The appearance of this coating in the as-received condition is shown in figure 19. The surface appearance was very uniform, light gray in color, and smooth in texture, but metallographic examination

indicated severe contamination of the substrate material with a continuous network of precipitates in the grain boundaries and through the grains.

The results of the room-temperature tensile tests (table III) show a severe loss in tensile elongation from 30 to 2 percent as a result of the coating application. The room-temperature strength was slightly higher than that in the uncoated condition and increased slightly after 1-hour exposure at 2400° F (1590° K). The elevated-temperature tensile test results in table IV show a strength increase of nearly 100 percent at 2000° F (1365° K) and 2400° F (1590° K) as compared with the uncoated material properties. The coated specimens had elongations of 9 and 25 percent, respectively, at 2000° F and 2400° F. These results suggest a strengthening mechanism which causes severe embrittlement at low temperatures. This mechanism is discussed in a later section. Bend ductility test results (table V) indicated a severe loss in ductility with all specimens tested failing in a brittle fracture.

Results of the oxidation tests at atmospheric pressure $\left(101 \ kN/m^2\right)$ are shown in figure 20 and the appearances of the exposed specimens are shown in figure 21. There was little damage at 2000° F (1365° K) before 140-hours exposure. At 2400° F (1590° K) severe damage began after approximately 30-hours exposure. At 2700° F (1755° K) tests were terminated from 1 to 24 hours.

Coating 7.- Coating 7 was applied by using similar techniques to those used in coating 6, but the resultant coating itself was only half as thick, 0.00081 inch (20 μm); thus, the temperature-time history for this coating was different than that used for coating 6. The X-ray emission data showed a much higher titanium intensity from the coating surface than for coating 6. The appearance of this coating shown in figure 22, along with metallurgical examination, indicates that the substrate was relatively unaffected for this coating cycle. The coating process reduced the room-temperature tensile elongation from 30 to 17 percent whereas other room-temperature tensile properties remained essentially unchanged (table III). After 1-hour exposure at 2400° F (1590° K), tensile properties increased slightly whereas elongation was further reduced to 10 percent. Elevated-temperature tensile test results show an unexplainably high ultimate stress at 2000° F (1365° K); however, a similar increase was not noted at 2400° F (1590° K) (table IV). Bend ductility tests of specimens of this coating in the as-coated condition indicated no loss in ductility, but specimens which were exposed at elevated temperatures and damaged by oxidation were severely embrittled (table V).

Results of the oxidation tests are shown in figure 23 and macro-photographs of exposed specimens are shown in figure 24. Oxidation protection afforded by this coating was poor, probably because the coating was relatively thin.

Coating 8.- Results of the X-ray study on coating 8 (table II) showed that this coating had the highest titanium intensity from the surface and also exhibited a high

silicon intensity, whereas the columbium intensity was lowest. The coating itself was the thickest coating investigated at 0.0034 inch (86 μm) and is shown in the as-received condition in figure 25. The coating was uniformly gray in color and somewhat rough in texture. Metallurgical examinations indicated some alteration of substrate in the form of precipitated particles and evidence of grain growth.

There was little or no effect on the room-temperature tensile strength in the as-coated condition or after 1- and 8-hours exposure at 2400° F, but elongation was reduced from 30 to 12 percent by the coating application and further reduced to 7 percent after 8-hours exposure at 2400° F (table III). Elevated-temperature tensile test results indicated a slight increase in ultimate tensile strength as compared with the uncoated material (table IV).

Results of the oxidation study at atmospheric pressure $\left(101 \text{ kN/m}^2\right)$ and also at reduced pressures are shown in figure 26 and macro-photographs of exposed specimens are shown in figure 27 for atmospheric pressure and in figure 28 for the reduced pressure tests. At 2000° F (1366° K) oxidation protection was good for a minimum of 140 hours. At 2400° F (1590° K) cyclic oxidation life was reduced to approximately 100 hours. Further reductions in lifetime were noted at 2700° F. The low-pressure test results indicate a very small mass change as shown in figure 26 with no visual evidence of failure.

Bend ductility tests on oxidation specimens showed severe embrittlement after 140 one-hour cycles, but there was no loss in ductility after 224 hours continuous testing at 2000° F (1365° K) (table V). There was little or no oxidation damage in either test. These results indicate that initial evidence of coating breakdown will not necessarily appear as oxidation damage but rather in severe loss of ductility. A mechanism for this embrittlement is discussed in the subsequent general comments section.

Coating 9.- The X-ray study on coating 9 resulted in identification of chromium, titanium, and silicon from the coating process with intensities as reported in table II; columbium and zirconium from the substrate were also identified. The primary compound was identified as a solid solution of $CrSi_2$ and $CbSi_2$. The appearance of coating 9 is shown in figure 29 in the as-received condition. The metallographic examinations revealed severe alteration of the base material by the coating process, with general precipitation of particles. The coating process did not cause appreciable grain growth.

Room-temperature tensile strength remained unchanged as a result of the coating process, but the substrate was completely embrittled. Elevated-temperature tensile test results showed a large increase in ultimate tensile strength, especially at 2400° F (table III). This strengthening effect was also observed for coating 6 and is discussed

subsequently. Bend test results also indicated a lack of ductility (table V). All tests resulted in brittle fracture of the specimen after very small deflections.

Results of the oxidation study at atmospheric $\left(101 \text{ kN/m}^2\right)$ pressure are presented in figure 30 and photographs of exposed specimens are shown in figure 31. Protection at 2000° F (1365° K) was good for a minimum of 140 hours, but protection at 2400° F (1590° K) was reduced somewhat. At 2700° F (1755° K) failures occurred after 4.3 and 45 hours.

Coating 10.- Results of the X-ray emission study on coating 10 indicated columbium, titanium, and zirconium in the coating. The X-ray diffraction analysis indicated that the primary compound was Al_3Cb (table II). This coating was the only aluminide coating investigated. Aluminum was not identified by emission technique because the low-energy X-rays are difficult to detect. The coating was relatively thin, 0.00133 inch (33 μm). (See table I.) The appearance of this coating is shown in figure 32 in the as-received condition. Metallographic examinations indicated that the substrate appeared to be relatively free of contamination but showed some evidence of grain-boundary precipitation. The room-temperature tensile properties were essentially unchanged by the coating process and there was only a negligible loss in elongation. The bend ductility tests (table V) showed no loss in ductility due to the coating application but specimens were generally embrittled after high-temperature exposure.

Oxidation data shown in figure 33 and macro-photographs of exposed specimens shown in figure 34 indicate that the coating provides limited oxidation protection, probably because of the thinness of the coating.

Coating 11.- Results of the X-ray study on coating 11 indicated columbium, titanium, silicon, and zirconium with moderate intensities, and a primary crystal structure of $CbSi_2$ (table II). The appearance of this coating in the as-received condition is shown in figure 35. The coating surface was speckled gray in color with a relatively rough texture. Metallographic studies indicated some slight grain growth and some precipitation in the substrate. The room-temperature tensile strength was unaffected by the coating process, but again the elongation as compared with that of the uncoated material was reduced from 30 to 14 percent after coating and to 4 percent after 8-hours exposure at 2400° F (table III). The elevated-temperature tensile data (table IV) show no significant change over the uncoated material.

Results of the oxidation study both at atmospheric pressure $\left(101 \text{ kN/m}^2\right)$ and at reduced pressures are shown in figure 36. Little damage was noted at 2000° F (1365° K) prior to 140-hours exposure. At 2400° F (1590° K) oxidation protection was lowered considerably to approximately 30 hours. This coating provided substrate protection from 6 to 55 hours at 2700° F (1755° K). Figures 37 and 38 show exposed specimens at

atmospheric pressure $\left(101 \text{ kN/m}^2\right)$ and at reduced pressures, respectively. It should be noted that there was no evidence of damage visually on the specimens tested at reduced pressures; however, specimens exposed at 0.5 torr $\left(67 \text{ N/m}^2\right)$ did appear to form a glassy surface layer. The bend-test results (table V) indicated that embrittlement does not begin until visible damage due to coating spall-off occurs which suggests that coating breakdown results in diffusion of oxygen into the substrate. All specimens exposed at low pressure had good bend ductility after 20 one-hour cycles.

Coating 12.- Results of the X-ray study on coating 12 indicate that this coating had the highest intensities of chromium and silicon relative to the other coatings and a high intensity of titanium (table II). Lower intensities of columbium and zirconium were also observed. The primary crystal structure was that of $CrSi_2$-$CbSi_2$ solid solution. Views of this coating in the as-received condition are shown in figure 39. This coating was also speckled gray in appearance and had a medium smooth texture. Metallographic examinations indicate no precipitates in the substrate. A well-defined diffused layer and considerable grain growth were evident after the coating process. Room-temperature tensile data indicate no change in tensile strength due to the coating application, but a decrease in elongation from 30 to 14 percent was observed (table III). Specimens exposed at 2400° F for 8 hours exhibited a further reduction in elongation to 4 percent. Elevated-temperature tensile tests (table IV) indicated that the ultimate strength was similar to that of the uncoated material and specimens of other coatings.

Oxidation data for this coating are shown in figure 40 for atmospheric pressure $\left(101 \text{ kN/m}^2\right)$ and reduced pressures. At atmospheric pressure the coated specimen exhibited no oxidation failures up to 240-hours exposure at 2000° F (1365° K); no failures were noted before 155-hours exposure at 2400° F (1590° K). At 2700° F (1755° K), however, failure of the cyclic specimens occurred within 2 to 3 hours. Continuously tested specimens at 2700° F provided protection from 20 to 100 hours. The results of the low pressure tests at 0.5 and 0.05 torr $\left(67 \text{ and } 6.7 \text{ N/m}^2\right)$ showed no evidence of failure from mass change indication. Appearance of exposed specimens is shown after exposure in figures 41 and 42.

The oxidation and bend-test results indicate that specimens of this coating exhibited embrittlement of the substrate when cyclically exposed, and showed no evidence of oxidation damage. After 240 one-hour cycles at 2000° F there was no visual evidence of failure and no mass changes of large magnitude; however, bend tests resulted in brittle fracture (table V). The specimen tested continuously for 240 hours at 2000° F was not embrittled. Reduced pressure tests at 0.05 torr resulted in severe embrittlement after 20 one-hour cycles at 2400° F with no obvious oxidation damage.

General Comments

X-ray analysis.- The X-ray emission analyses of the coated specimens were all made under the same conditions so that semi-quantitative comparisons could be made concerning relative percentages of a given element for all the coatings. It should be noted that different elements cannot be compared without a mathematical analysis or comparison with other standards. Most coatings consisted primarily of $CbSi_2$ or $CbSi_2$-$CrSi_2$ solid solution. Alloying elements in the coatings are apparently present as substitutional atoms as deduced from a change in interplanar spacing from X-ray diffraction data.

Tensile test results.- The results of the room-temperature and elevated-temperature tensile tests indicated that the most severely affected property was tensile elongation. All the coatings affected the substrate elongation to some degree, but specimens of coatings 12, 11, 8, 5, and 4 exhibited some ductility at both room-temperature and after certain high-temperature exposures. On the other hand, coatings 12 and 8 appear to be limited in usefulness by substrate embrittlement rather than by oxidation when exposed cyclically, and low pressure tests indicate this "embrittlement life" to be less than 20 hours at 2400° F (1590° K) in some cases. Little change was observed in the room-temperature tensile strength and modulus of almost all coatings. However, coatings which were completely embrittled (coatings 2 and 6) by the coating process also had increased high-temperature tensile strength, up to twice as much as the uncoated alloy. This phenomenon may possibly be controlled by the zirconium percentage in the base material. The same effect may not be observed in other alloys. The increasing scatter in the data with increasing exposure time may be due in part to oxidation damage on some of the coated specimens. The variation in elastic modulus is due in part to the inaccuracy of determination of the load-bearing cross-sectional area because of the coating process, but observed changes in substrate microstructure indicate that the increase in modulus for coating 2 is a true property change. The curves in figure 1 are shown to indicate only general trends since few tests were made for each coating in the as-received condition. Tests were made on both longitudinal and transverse specimens of coated and uncoated material, and no grain orientation effect was observed.

Oxidation.- Generally, the modified silicides containing chromium and titanium appear to provide the most favorable resistance to oxidation although specific details of the protective mechanism remain unexplained. Several of the coatings investigated indicated a potential for providing oxidation resistance in thermal protection systems at temperatures up to 2400° F (1590° K). Oxidation protection was unpredictable for all the coatings investigated at 2700° F (1755° K). The primary cause of cyclic oxidation damage for the coatings which provided longest protection for the substrate (coatings 12,

8, 11, 4, and 5) appeared to be coating spall-off caused by thermal expansion mismatch between coating and substrate. It should be noted that nearly all failures initiated on edges or around holes where the thermal expansion difference would have the most pronounced effect. From the cyclic oxidation test data it appeared that the Cr-Ti modified silicide coatings were more compatible with the substrate in regard to thermal expansion.

There is also indication that oxygen diffusion can occur through the substrate during cyclic exposures at temperatures as low as 2000° F (1365° K) and affect the mechanical properties of the material without visual evidence of general coating breakdown. For the modified silicide coatings which provided better oxidation protection, it was found that substrate embrittlement could possibly be the limiting factor for the usefulness of the coated columbium alloy sheet. A possible mechanism for this embrittlement is described in a later section.

Results of the low-pressure oxidation tests showed that a mass loss occurred only on the first cycle. A portion of this mass loss could have been caused by chromium evaporation in several of the coatings at the test temperature. Chromium vapor pressure is relatively high, and at the pressures utilized, the chromium could have evaporated. After a slight mass loss on the initial cycle, all specimens showed a gradual mass gain which would appear to indicate gaseous pickup resulting in formation of oxides of silicon, chromium, and zirconium in coating and substrate. Studies of this type at higher flow rates are of importance for detailing coating behavior over the entire range of conditons which may be encountered in hypersonic flights. Equipment limitations precluded such studies in this investigation.

Substrate embrittlement.- During this investigation severe substrate embrittlement appeared to be a contributing factor in degrading the usefulness of coating-substrate systems of the type described herein. The coating process itself can cause severe embrittlement of substrate, as noted for coatings 2, 6, and 9. Photomicrographs of a specimen of coating 6 are shown in the as-received condition in figure 43. This coating caused severe embrittlement of the substrate. The photomicrographs shown represent an area which was examined with an electron probe X-ray microanalyzer. Exposure under the influence of an electron beam causes fluorescence of the grain boundaries as shown in figure 43 and suggests a nonmetallic precipitate in or adjacent to the grain boundaries. Figure 44 shows an electron microprobe trace for zirconium and thus indicates the high relative intensity of zirconium within the grain boundaries. Substrate embrittlement can also be caused by subsequent high-temperature exposure after a coating process which has not resulted in embrittlement. In both coatings 8 and 12, bend-test results were quite different with regard to cyclic and continuous exposure. Coating 8 exhibited a ductile bend after 225-hours continuous exposure at 2000° F (1365° K), but after 140 one-hour cycles at 2000° F the bend test resulted in a brittle fracture.

15

Similarly, coating 12 exhibited a ductile bend after 240-hours continuous exposure but failed with a brittle fracture after 240 one-hour cycles. None of these specimens had extensive oxidation damage, and the coating 12 specimens had no visual evidence of damage whatsoever. Figure 45 shows a cross section of a specimen of coating 12 which underwent a 90° bend after 240-hours continuous testing at 2000° F. Figures 46(a) and 46(b) show a cross section of a specimen of coating 12 bend tested after 240 one-hour cycles at 2000° F, and exhibiting intergranular failure across the specimen. Electron microprobe studies have indicated large concentrations of zirconium present in inclusions and also in the grain boundaries, as was observed for coating 6 in the as-received condition. The same fluorescence effect was observed for the coating 12 specimen cycled for 240 hours, as shown in figure 46(c). Zirconium traces for this specimen were similar to that shown in figure 44. It should be noted that specimens which were not embrittled showed no grain-boundary fluorescence under the electron beam and no increase in zirconium concentration at grain boundaries. These factors in conjunction with the strong chemical affinity of zirconium for oxygen suggest that these precipitates are ZrO_2. The foregoing suggests that during thermal cycling, microscopic cracks develop in the coatings and allow oxygen diffusion to occur into the substrate. Similar results were not observed during continuous testing. For extreme cases this embrittlement phenomenon could be the limiting factor in determining the usefulness of certain coating systems in the 2000° F to 2400° F range (1365° K to 1590° K).

Substrate recession studies.- Results of the tests to study solid-state diffusion and substrate recession rate are shown in figure 47. The results indicate a substrate recession from 0.0005 to 0.001 inch (12 to 25 μm) in 50 hours at 2500° F compared with 0.001 to 0.002 (25 to 50 μm) for molybdenum from reference 12. The fact that there was no difference in recession rates when exposed in air and argon indicates that the recession is due to solid-state diffusion of constituents only in the substrate coating system. However, this low surface recession rate does not preclude the possibility of oxygen diffusion through the coating into the substrate which might not be observable under the microscope and which was observed indirectly by microprobe analysis. It, therefore, seems that the problem of diffusion will be primarily one of grain-boundary diffusion with an embrittling effect rather than one of substrate thickness decrease.

CONCLUSIONS

From the results of a study of 12 oxidation-resistant coatings on columbium, 10-percent titanium, 5-percent zirconium alloy sheet, the following statements may be made:

16

1. It appeared that an upper limit for protection of this alloy from oxidation with some degree of consistency was approximately 2400° F (1590° K) if modified silicide coatings containing titanium and chromium are used.

2. The usefulness of thin-gage coated columbium alloy sheet may be determined by substrate embrittlement rather than by oxidation failures in some high-temperature applications.

3. Room-temperature tensile tests indicated no significant changes in tensile properties with the exception of tensile elongation which in all cases was lowered and in three coatings was severely reduced. In these three embrittled coatings, elevated-temperature tensile strength was increased, apparently by the same mechanism which caused embrittlement.

4. Cyclic oxidation exposure resulted in embrittlement of some of the coated specimens at temperatures as low as 2000° F (1365° K). Under similar conditions, continuous oxidation exposure did not produce embrittlement.

5. The embrittlement of the Cb—10-percent Ti—5-percent Zr alloy substrate appeared to be caused by the diffusion of oxygen through microcracks in the coating into the substrate with subsequent formation of ZrO_2 in or adjacent to the grain boundaries. Bend-test failures were noted to be intergranular.

6. Cyclic oxidation testing at 0.5 and 0.05 torr (67 N/m^2 and 6.7 N/m^2) at low mass flow rates resulted in mass gains after the first cycle and indicated gaseous pickup and subsequent formation of stable oxides of silicon, chromium, and/or zirconium.

7. Substrate thickness loss due to solid-state diffusion did not appear to be a significant factor for high-temperature utilization of these coatings.

Langley Research Center,
National Aeronautics and Space Administration,
Langley Station, Hampton, Va., October 5, 1965.

APPENDIX A

CONVERSION OF U.S. CUSTOMARY UNITS TO SI UNITS

The International System of Units (SI) was adopted by the Eleventh General Conference on Weights and Measures, Paris, October 1960, in Resolution No. 12 (ref. 9). Conversion factors for the units used herein are given in the following table:

Physical quantity	U.S. Customary Units	Conversion factor (a)	SI Unit
Length	in.	0.0254	meters (m)
Temperature	$(^\circ F + 459.67)$	5/9	degrees Kelvin $(^\circ K)$
Volume flow	ft^3/hr	0.79×10^{-5}	cubic meters per second (m^3/s)
Stress	$psi = lbf/in^2$	6.895×10^3	newtons per square meter (N/m^2)
Young's modulus	$psi = lbf/in^2$	6.895×10^3	newtons per square meter (N/m^2)
Pressure	$torr = mm Hg$	133	newtons per square meter (N/m^2)

[a]Multiply value given in U.S. Customary Unit by conversion factor to obtain equivalent value in SI unit.

Prefixes to indicate multiple of units are as follows:

Prefix	Multiple
kilo (k)	10^3
mega (M)	10^6
centi (c)	10^{-2}
milli (m)	10^{-3}

REFERENCES

1. Bartlett, E. S.; and Houck, J. A.: Physical and Mechanical Properties of Columbium and Columbium-Base Alloys. DMIC Rept. 125, Battelle Mem. Inst., Feb. 22, 1960.

2. Schmidt, F. F.; and Ogden, H. R.: The Engineering Properties of Columbium and Columbium Alloys. DMIC Rept. 188, Battelle Mem. Inst., Sept. 6, 1963.

3. Gerken, J. M.; and Fullerton, T. L.: Investigation of Weldability of Additional Columbium Alloys. ASD-TDR-63-843, U.S. Air Force, Oct. 1963.

4. Welty, J. W.; Valdez, P. J.; Smeltzer, C. E., Jr.; and Davis, C. P.: Joining of Refractory Metal Foils. ASD-TDR-63-799, Pt. I, U.S. Air Force, July 1963.

5. McCown, J. W.; Wilks, C. R.; Gagola, L. J.; Norton, A.; and Schwartz, M.: Final Report on Manufacturing Methods and Design Procedures of Brazed Refractory Metal Honeycomb Sandwich Panels. ASD-TDR-63-767, U.S. Air Force, Nov. 1963.

6. Wichorek, Gregory R.; and Stein, Bland A.: Experimental Investigation of Insulating Refractory-Metal Heat-Shield Panels. NASA TN D-1861, 1964.

7. Moore, V. S.; and Stetson, A. R.: Evaluation of Coated Refractory Metal Foils. RTD-TDR-63-4006, Pt. I, U.S. Air Force, Sept. 1963.

8. Aves, William L., Jr.; Bourland, Gordon W.; Featherston, Aleck B.; Forcht, Brennan A.; and O'Kelly, Kent P: Diffusion Coating Process for Columbium Base Alloys. ASD-TDR-62-333, U.S. Air Force, Feb. 1962.

9. Mechtly, E. A.: The International System of Units — Physical Constants and Conversion Factors. NASA SP-7012, 1964.

10. Manning, Charles R., Jr.; Royster, Dick M.; and Braski, David N.: An Investigation of a New Nickel Alloy Strengthened by Dispersed Thoria. NASA TN D-1944, 1963.

11. Rummler, Donald R.; Stein, Bland A.; and Pride, Richard A.: A Study of Several Oxidation-Resistant Coatings on Mo-0.5Ti Alloy Sheet at 2500° F. NASA TN D-2040, 1964.

12. Stein, Bland A.; and Lisagor, W. Barry: Diffusion Studies of Several Oxidation Resistant Coatings on Mo-0.5Ti Molybdenum Alloy at 2500° F. NASA TN D-2039, 1964.

TABLE I.- IDENTIFICATION OF THE VARIOUS COATINGS INCLUDED IN

THIS INVESTIGATION AND METHODS OF APPLICATION

Coating	Coating thickness, in. (μm)	Method of application	Supplier
1	0.00154 (39.2)	Two cycle, pack cementation.	American Machine & Foundry Co.
2	.00309 (78.5)	Three cycle, pack cementation.	American Machine & Foundry Co.
3	.00196 (49.8)	Two cycle, pack cementation: first cycle, silicon, second cycle, chromium boron.	Ling-Temco-Vought, Inc.
4	.00146 (37.1)	One cycle fluidized bed, silicon.	Boeing Airplane Co.
5	.00152 (38.6)	First cycle, fluidized bed, silicon; second cycle, sprayed SiC one side only.	Boeing Airplane Co.
6	.00163 (41.5)	First cycle, vapor deposition titanium chromium; second cycle, fluidized bed, modified silicide.	E. I. DuPont de Nemours
7	.00081 (20.6)	First cycle, vapor deposition titanium chromium; second cycle, fluidized bed, modified silicide.	E. I. DuPont de Nemours
8	.00342 (86.9)	Two cycle, pack cementation: first cycle, vacuum pack cementation, titanium; second cycle, pack cementation, silicon.	General Telephone & Electronics Corp.
9	.00240 (61.0)	Three cycle, pack cementation: first cycle, chromium-titanium; second and third cycles, silicon-carbon-tantalum.	General Technologies Corp.
10	.00133 (33.8)	One cycle, slurry coating, aluminum; inert-gas heat treatment.	North American Aviation, Inc.
11	.00311 (79.1)	One cycle, pack cementation, alloyed silicide.	Pfaudler Co.
12	.00197 (50.1)	Two cycle, pack cementation: first cycle, prealloyed chromium-titanium; second cycle, silicon.	Thompson Ramo Wooldridge, Inc.

TABLE II.- X-RAY STUDY OF THE 12 COATINGS INVESTIGATED ON Cb-10Ti-5Zr ALLOY SHEET

Coating	Emission								Diffraction	Remarks
	Relative intensity[a] (counts per second) and characteristic X-ray line of —								Primary compound	
	Cb, $K_\alpha III$	Ti, $K_\alpha II$	Cr, $K_\alpha I$	Fe, $K_\alpha I$	Si, $K_\alpha I$	Zr, $K_\alpha II$	K, $K_{\beta_1}I$	Co, $K_\alpha I$		
1	40	77	7	51	20	20	--	---	CbB_2	
2	41	30	3	28	36	20	--	---	CbB_2	
3	33	47	12	9	29	13	26	---	$CbSi_2$-Cb_5Si_3	
4	43	44	6	--	132	16	--	6	$CbSi_2$	
5	41	51	--	9	170	19	--	6	$CbSi_2$ (SiC)	One side, SiC overcoat
6	25	30	41	2	98	11	--	---	$CbSi_2$-$CrSi_2$	Solid solution
7	35	154	15	--	39	13	--	---	$CbSi_2$	
8	18	190	--	--	165	--	--	---	$CbSi_2$	
9	33	26	44	--	50	14	--	---	$CbSi_2^2$-$CrSi_2$	Solid solution
10	36	63	--	--	--	18	--	---	Al_3Cb	
11	31	28	--	--	50	14	--	---	$CbSi_2$	
12	18	135	61	--	180	4	--	---	$CrSi_2$-$CbSi_2$	Solid solution

[a] Cr K_α radiation used for Si, Ti, K; Pt K_α radiation used for others.

TABLE III.- ROOM-TEMPERATURE TENSILE PROPERTIES OF COATED Cb-10Ti-5Zr ALLOY SHEET AS-RECEIVED AND AFTER VARIOUS EXPOSURES AT 2400° F (1589° K) IN AIR[a]

Coating	Ultimate tensile strength, ksi (MN/m^2)			Tensile yield strength, ksi (MN/m^2)			Young's modulus, psi (GN/m^2)			Percent elongation in 1 inch (2.54 cm)		
	As-received	1-hr exposure	8-hr exposure	As-received	1-hr exposure	8-hr exposure	As-received	1-hr exposure	8-hr exposure	As-received	1-hr exposure	8-hr exposure
Uncoated	76.0 (525)	82.5 (569)	73.0 (504)	65.8 (454)	77.5 (535)	69.2 (478)	14.6×10^6 (101)	15.3×10^6 (106)	15.2×10^6 (105)	30	27	25
1	79.0 (545)	(b)	(b)	67.5 (466)	(b)	(b)	15.2 (105)	(b)	(b)	14		
2	48.7 (336)	(b)	(b)	(c)	(b)	(b)	23.9 (165)	(b)	(b)	0		
3	78.1 (539)	78.9 (544)	60.0 (414)	66.5 (459)	67.0 (462)		15.0 (103)	16.0 (110)	15.2 (105)	19	0	0
4	75.8 (523)	76.3 (526)	65.0 (448)	59.0 (407)		64.0 (441)	14.9 (103)	13.0 (89.6)	13.6 (938)	20	12	16
5	76.3 (526)	73.4 (506)	69.9 (482)	64.2 (443)	64.2 (443)	67.0 (462)	15.8 (109)	14.6 (101)	15.0 (103)	21	20	11
6	82.5 (569)	94.0 (648)	67.0 (462)	74.5 (514)	83.6 (576)	65.0 (448)	15.7 (108)	15.0 (103)	14.6 (101)	2	3	3
7	85.6 (591)	98.2 (677)	(b)		81.7 (564)	(b)	15.0 (103)	17.5 (121)	(b)	17	10	(b)
8	80.2 (553)	73.3 (506)	72.7 (501)	64.8 (447)	63.0 (435)	67.6 (467)	16.4 (113)	16.5 (114)	12.6 (86.9)	12	14	7
9	72.9 (503)	65.5 (452)	62.6 (432)	63.8 (440)	64.2 (443)		15.3 (106)	14.8 (102)	14.8 (102)	0	0	0
10	78.6 (543)	(d)	(b)	65.5 (452)	(d)	(b)	14.0 (96.6)	(d)	(b)	27	(d)	(b)
11	73.0 (504)	74.4 (513)	48.2 (332)	59.6 (411)	60.2 (415)	48.0 (331)	16.6 (114)	16.6 (114)	13.3 (91.7)	14	(e)	4
12	77.7 (536)	80.0 (551)	79.6 (549)	71.6 (494)	65.0 (448)	79.0 (545)	15.4 (106)	15.9 (110)	15.3 (105)	14	14	4

[a]Uncoated material exposed in vacuum and tested in argon.
[b]Failed by oxidation.
[c]Failed before yield.
[d]Broke on insertion into grip.
[e]Not determined.

21

TABLE IV.- TENSILE PROPERTIES OF COATED Cb-10Ti-5Zr ALLOY

AT 2000° F (1366° K) AND 2400° F (1589° K) IN AIR

Coating	Temperature, °F (°K)	Ultimate tensile strength, ksi (MN/m^2)	Percent elongation in 1 inch (2.54 cm)
Uncoated[a]	2030 (1383)	24 (168)	11
	2480 (1633)	9 (66)	4
1	2000 (1366)	31 (214)	6
	2400 (1589)	11 (82)	13
2	2000 (1366)	23 (164)	0
	2400 (1589)	16 (114)	4
3	2000 (1366)	27 (188)	3
	2400 (1589)	12 (86)	15
4	2000 (1366)	26 (184)	19
	2400 (1589)	13 (94)	38
5	2000 (1366)	28 (198)	14
	2400 (1589)	13 (90)	29
6	2000 (1366)	41 (284)	9
	2400 (1589)	19 (134)	25
7	2000 (1366)	45 (310)	18
	2400 (1589)	14 (103)	29
8	2000 (1366)	22 (156)	6
	2400 (1589)	12 (87)	17
9	2000 (1366)	31 (214)	7
	2400 (1589)	19 (133)	16
10	2000 (1366)	30 (211)	28
	2400 (1589)	11 (77)	20
11	2000 (1366)	29 (200)	8
	2400 (1589)	12 (87)	12
12	2000 (1366)	24 (168)	19
	2400 (1589)	11 (81)	27

[a]Tested in argon.

Coating	Type of test	Exposure temperature, °F (°K)	Exposure pressure, mm Hg (kN/m²)		Exposure time, hours	Maximum deflection, in. (cm)	Appearance after oxidation tests
Uncoated		As-received				0.475 (1.21)	
1		As-received				.425 (1.08)	
1	Continuous	2000 (1366)	760	(101)	100	.048 (.122)	Visible oxidation product
1	Cyclic	2000 (1366)	760	(101)	23	.300 (.762)	Visible oxidation product
1	Continuous	2400 (1589)	760	(101)	1	.050 (.127)	Visible oxidation product
1	Continuous	2700 (1755)	760	(101)	.15	.475 (1.21)	Extensive reaction
2		As-received				.075 (.191)	
2	Continuous	2000 (1366)	760	(101)	69	.063 (.160)	Visible oxidation product
2	Cyclic	2000 (1366)	760	(101)	21	.088 (.224)	Visible oxidation product
2	Continuous	2400 (1589)	760	(101)	1	.045 (.114)	Extensive oxidation product
2	Cyclic	2400 (1589)	760	(101)	4	.065 (.165)	Extensive oxidation product
2	Continuous	2700 (1755)	760	(101)	.2	.158 (.401)	Extensive reaction
2	Continuous	2700 (1755)	760	(101)	.1	.070 (.178)	Extensive reaction
2	Continuous	2700 (1755)	760	(101)	.25	.183 (.465)	Extensive reaction
3		As-received				.425 (1.08)	
3	Continuous	2000 (1366)	760	(101)	240	.300 (.762)	Visible oxidation product
3	Cyclic	2000 (1366)	760	(101)	130	.300 (.762)	Visible oxidation product
3	Continuous	2400 (1589)	760	(101)	42	.300 (.762)	Visible oxidation product
3	Cyclic	2400 (1589)	760	(101)	9	.275 (.698)	Oxidation damage
3	Continuous	2700 (1755)	760	(101)	.9	.300 (.762)	Visible oxidation product
3	Continuous	2700 (1755)	760	(101)	2.9	.300 (.762)	Visible oxidation product
4		As-received				.500 (1.27)	No failure
4	Continuous	2000 (1366)	760	(101)	140	.045 (.114)	Extensive oxidation damage
4	Cyclic	2000 (1366)	760	(101)	125	.095 (.241)	Extensive oxidation damage
4	Continuous	2400 (1589)	760	(101)	62	.095 (.241)	Extensive oxidation damage
4	Cyclic	2400 (1589)	760	(101)	54	.500 (1.27)	No failure
4	Cyclic	2400 (1589)	760	(101)	29	.500 (1.27)	Slight oxidation on edge
4	Cyclic	2400 (1589)	.5	(0.067)	20	.500 (1.27)	No visible damage
4	Cyclic	2400 (1589)	.5	(0.067)	20	.500 (1.27)	No visible damage
4	Cyclic	2400 (1589)	.05	(0.0067)	20	.500 (1.27)	No visible damage
4	Cyclic	2400 (1589)	.05	(0.0067)	20	.500 (1.27)	No visible damage
4	Cyclic	2700 (1755)	760	(101)	9	.475 (1.21)	Visible oxidation product
4	Cyclic	2700 (1755)	760	(101)	1	.075 (.191)	Extensive oxidation damage
5		As-received				.500 (1.27)	No failure
5	Cyclic	2000 (1366)	760	(101)	92	.500 (1.27)	Visible oxidation product
5	Cyclic	2400 (1589)	760	(101)	35	.500 (1.27)	Visible oxidation product
6		As-received				.275 (.698)	
6	Continuous	2000 (1366)	760	(101)	240	.100 (.254)	
6	Cyclic	2000 (1366)	760	(101)	144	.075 (.191)	
6	Cyclic	2400 (1589)	760	(101)	24	.100 (.254)	
6	Cyclic	2400 (1589)	760	(101)	75	.500 (1.27)	
6	Continuous	2700 (1755)	760	(101)	4.5	.300 (.762)	
6	Cyclic	2700 (1755)	760	(101)	1	.200 (.508)	
7		As-received				.500 (1.27)	
7	Continuous	2000 (1366)	760	(101)	113	.030 (.076)	Visible oxidation damage
7	Cyclic	2000 (1366)	760	(101)	42	.100 (.254)	Oxidation damage
7	Continuous	2400 (1589)	760	(101)	6	.500 (1.27)	Oxidation damage
7	Cyclic	2400 (1589)	760	(101)	4	.475 (1.21)	Oxidation damage
7	Cyclic	2400 (1589)	760	(101)	7	.475 (1.21)	Oxidation damage

Coating	Type of test	Exposure temperature, °F (°K)	Exposure pressure, mm Hg (kN/m²)		Exposure time, hours	Maximum deflection, in. (cm)	Appearance after oxidation tests
8		As-received				.500 (1.27)	
8	Continuous	2000 (1366)	760	(101)	224	.500 (1.27)	Oxidation on edges
8	Cyclic	2000 (1366)	760	(101)	140	.038 (.096)	Oxidation on edges
8	Continuous	2400 (1589)	760	(101)	180	.030 (.076)	Oxidation damage
8	Cyclic	2400 (1589)	760	(101)	125	.088 (.224)	Oxidation damage
8	Cyclic	2400 (1589)	760	(101)	126	.038 (.096)	Oxidation damage
8	Cyclic	2400 (1589)	.5	(0.067)	20	.500 (1.27)	No visible damage
8	Cyclic	2400 (1589)	.5	(0.067)	20	.500 (1.27)	No visible damage
8	Cyclic	2400 (1589)	.05	(0.0067)	20	.500 (1.27)	
8	Cyclic	2400 (1589)	.05	(0.0067)	20	.500 (1.27)	
9		As-received				0.098 (0.249)	
9	Continuous	2000 (1366)	760	(101)	220	.105 (.266)	
9	Cyclic	2000 (1366)	760	(101)	144	.105 (.266)	
9	Continuous	2400 (1589)	760	(101)	96	.038 (.096)	
9	Cyclic	2400 (1589)	760	(101)	54	.048 (.122)	
9	Continuous	2700 (1755)	760	(101)	4	.070 (.178)	
9	Cyclic	2700 (1755)	760	(101)	5	.045 (.114)	
10		As-received				.500 (1.27)	
10	Cyclic	2000 (1366)	760	(101)	16	.038 (.096)	Oxidation damage
10	Continuous	2400 (1589)	760	(101)	46	.075 (.191)	Oxidation damage
10	Cyclic	2400 (1589)	760	(101)	6	.475 (1.21)	Oxidation damage
10	Cyclic	2400 (1589)	760	(101)	5	.225 (.571)	Oxidation damage
11		As-received				.500 (1.27)	
11	Continuous	2000 (1366)	760	(101)	232	.100 (.254)	Oxidation damage
11	Cyclic	2000 (1366)	760	(101)	140	.500 (1.27)	Oxidation damage
11	Continuous	2400 (1589)	760	(101)	40	.250 (.635)	Oxidation damage
11	Cyclic	2400 (1589)	760	(101)	49	.500 (1.27)	Oxidation damage
11	Cyclic	2400 (1589)	760	(101)	28	.063 (.160)	Oxidation damage
11	Cyclic	2400 (1589)	.5	(0.067)	20	.500 (1.27)	No visible damage
11	Cyclic	2400 (1589)	.5	(0.067)	20	.500 (1.27)	No visible damage
11	Cyclic	2400 (1589)	.05	(0.0067)	20	.500 (1.27)	No visible damage
11	Continuous	2700 (1755)	760	(101)	53	.475 (1.21)	Visible glassy surface
11	Continuous	2700 (1755)	760	(101)	5.3	.475 (1.21)	Some edge damage
11	Cyclic	2700 (1755)	760	(101)	12	.500 (1.27)	Some edge damage
11	Cyclic	2700 (1755)	760	(101)	8	.500 (1.27)	Some edge damage
12		As-received				.500 (1.27)	
12	Continuous	2000 (1366)	760	(101)	240	.500 (1.27)	No visible damage
12	Cyclic	2000 (1366)	760	(101)	240	.063 (.160)	No visible damage
12	Cyclic	2400 (1589)	760	(101)	183	.090 (.228)	Oxidation damage
12	Cyclic	2400 (1589)	760	(101)	155	.300 (.762)	Oxidation damage
12	Cyclic	2400 (1589)	.5	(0.067)	20	.500 (1.27)	Visible coat breakdown
12	Cyclic	2400 (1589)	.5	(0.067)	20	.500 (1.27)	Visible coat breakdown
12	Cyclic	2400 (1589)	.05	(0.0067)	20	.028 (.071)	Visible coat breakdown
12	Cyclic	2400 (1589)	.05	(0.0067)	20	.022 (.056)	Visible coat breakdown
12	Cyclic	2400 (1589)	.05	(0.0067)	20	.033 (.084)	Visible coat breakdown
12	Cyclic	2400 (1589)	.05	(0.0067)	20	.025 (.063)	Visible coat breakdown
12	Cyclic	2700 (1755)	760	(101)	2	.500 (1.27)	Oxidation damage on edge
12	Cyclic	2700 (1755)	760	(101)	3	.500 (1.27)	Oxidation damage on edge
12	Cyclic	2700 (1755)	760	(101)	3	.500 (1.27)	
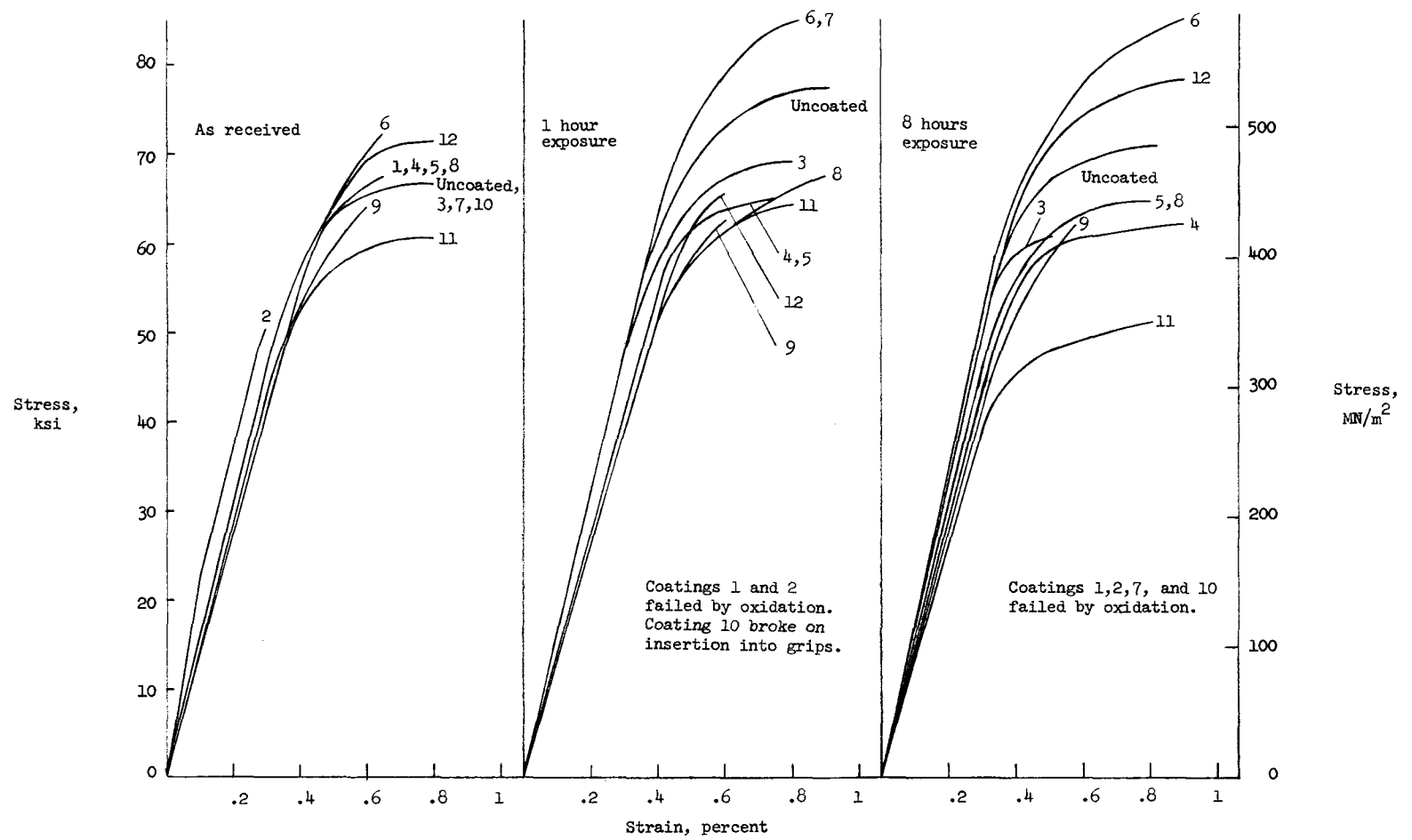
Figure 1.- Room-temperature stress-strain curves for coated and uncoated specimens of Cb-10Ti-5Zr alloy sheet as received and after various exposures at 2400° F (1590° K) in air for coated specimens or in vacuum for uncoated specimens.
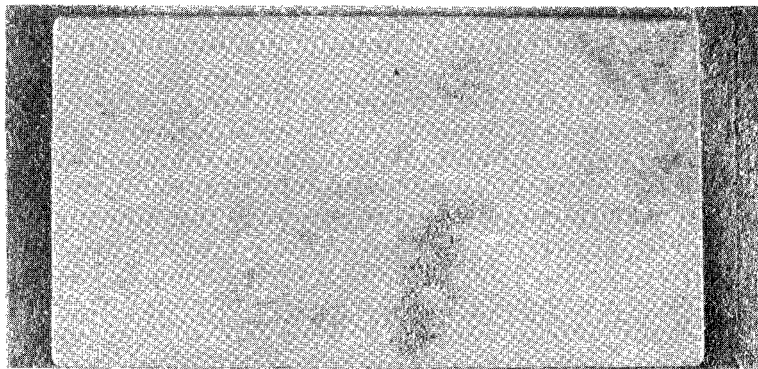
(a) As-coated appearance, X 2.
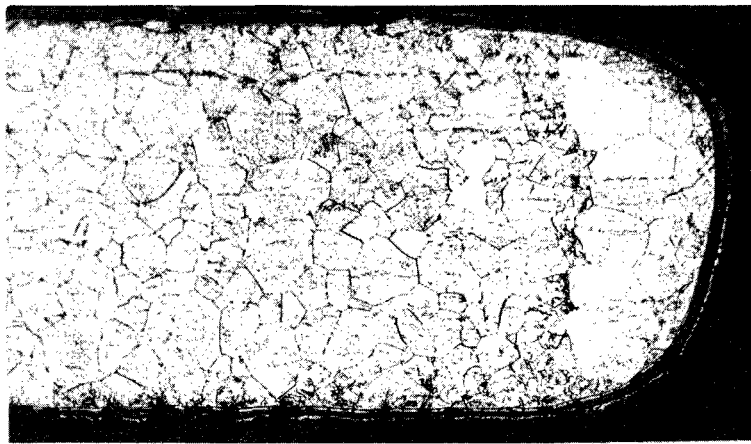
(b) Cross section, X 100.
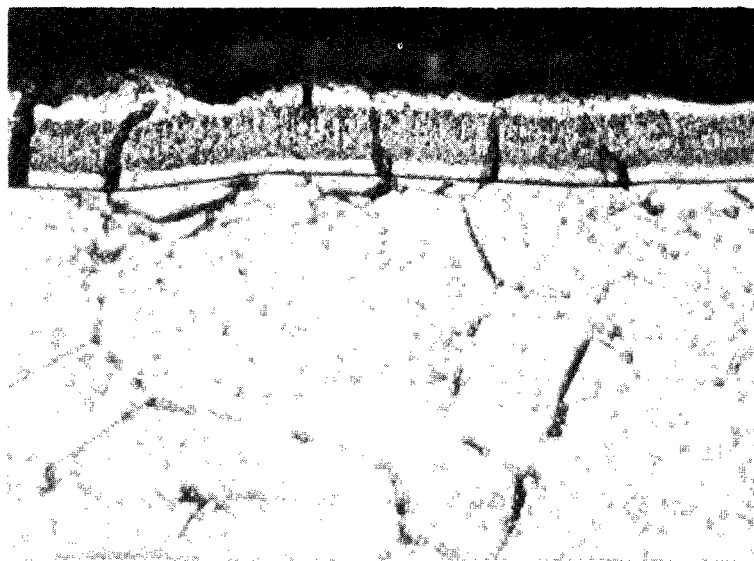
(c) Cross section, X 500.   L-65-7974

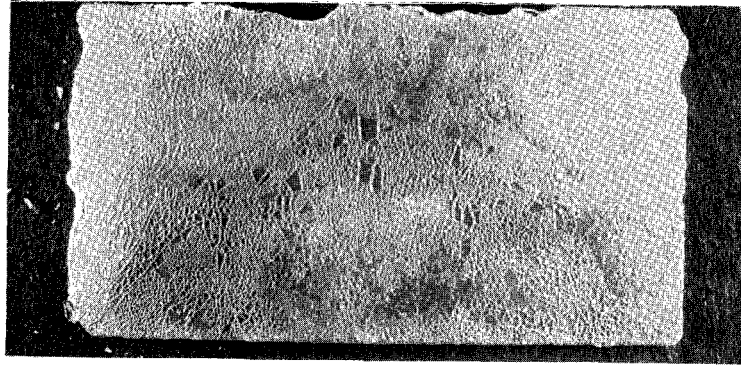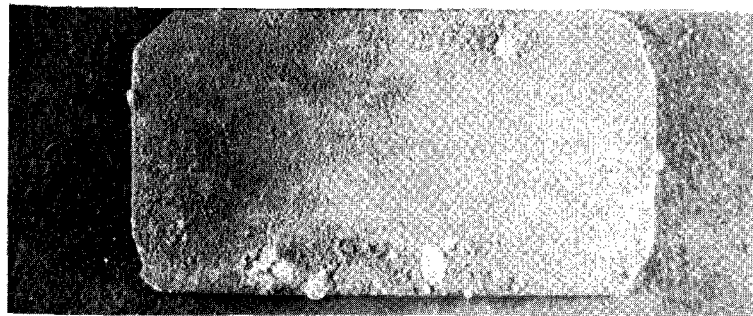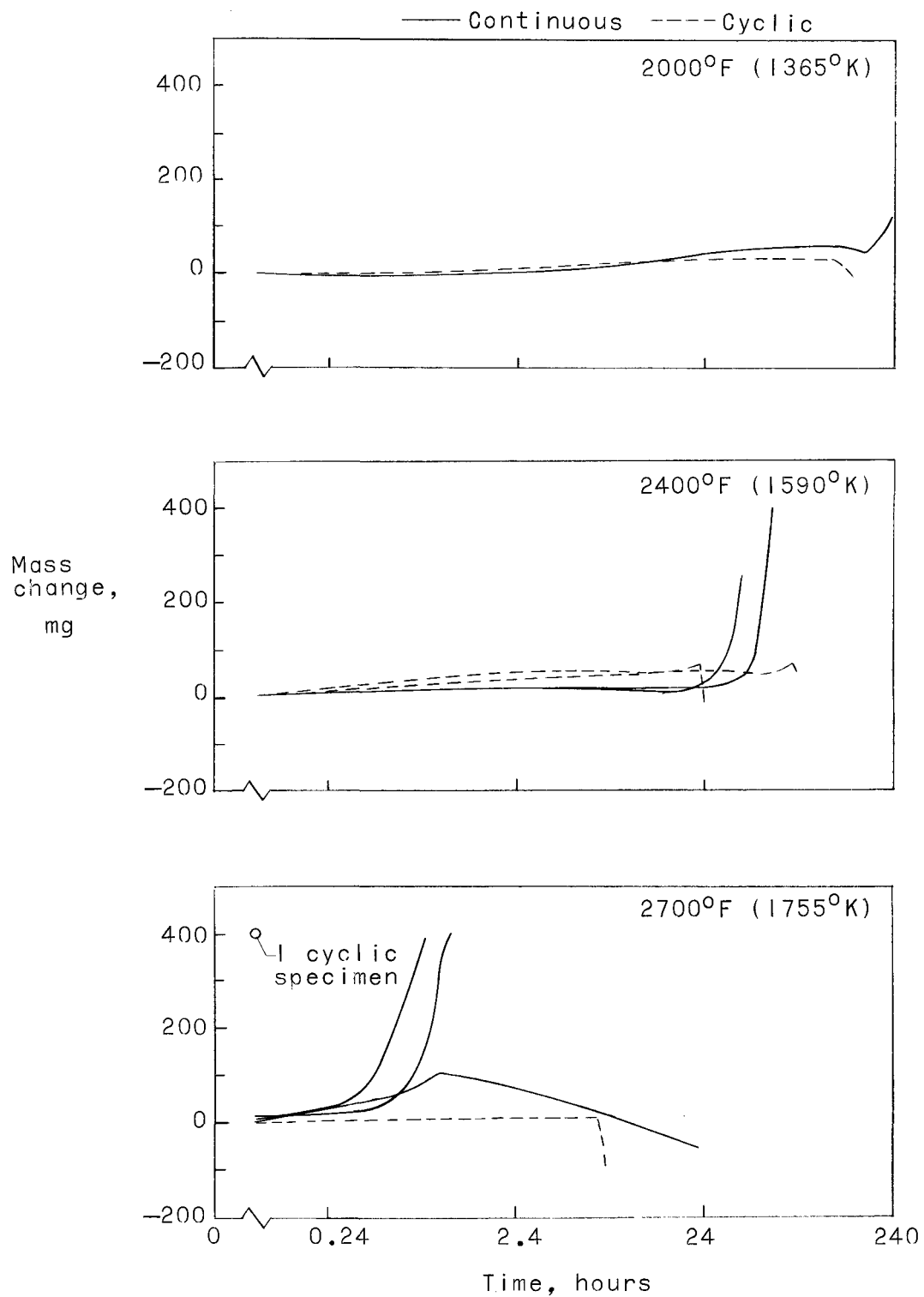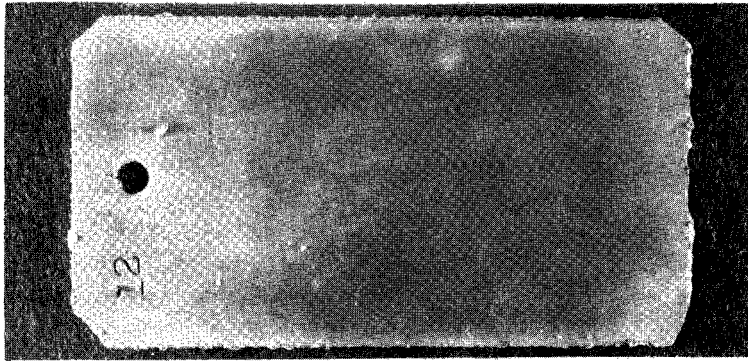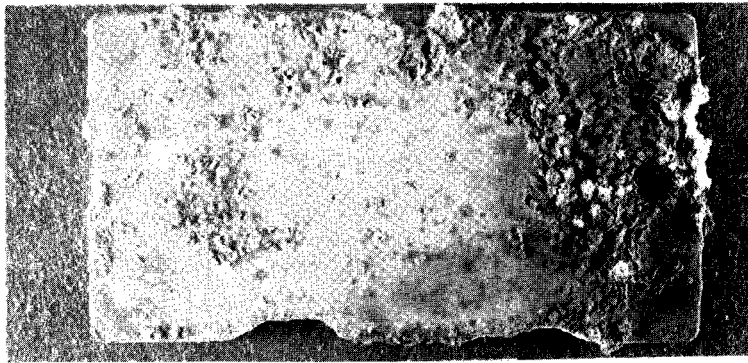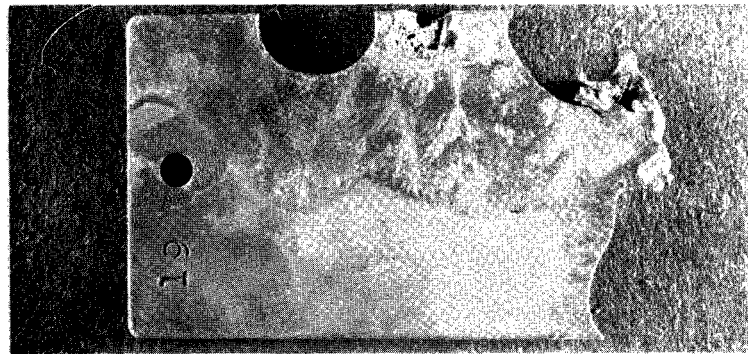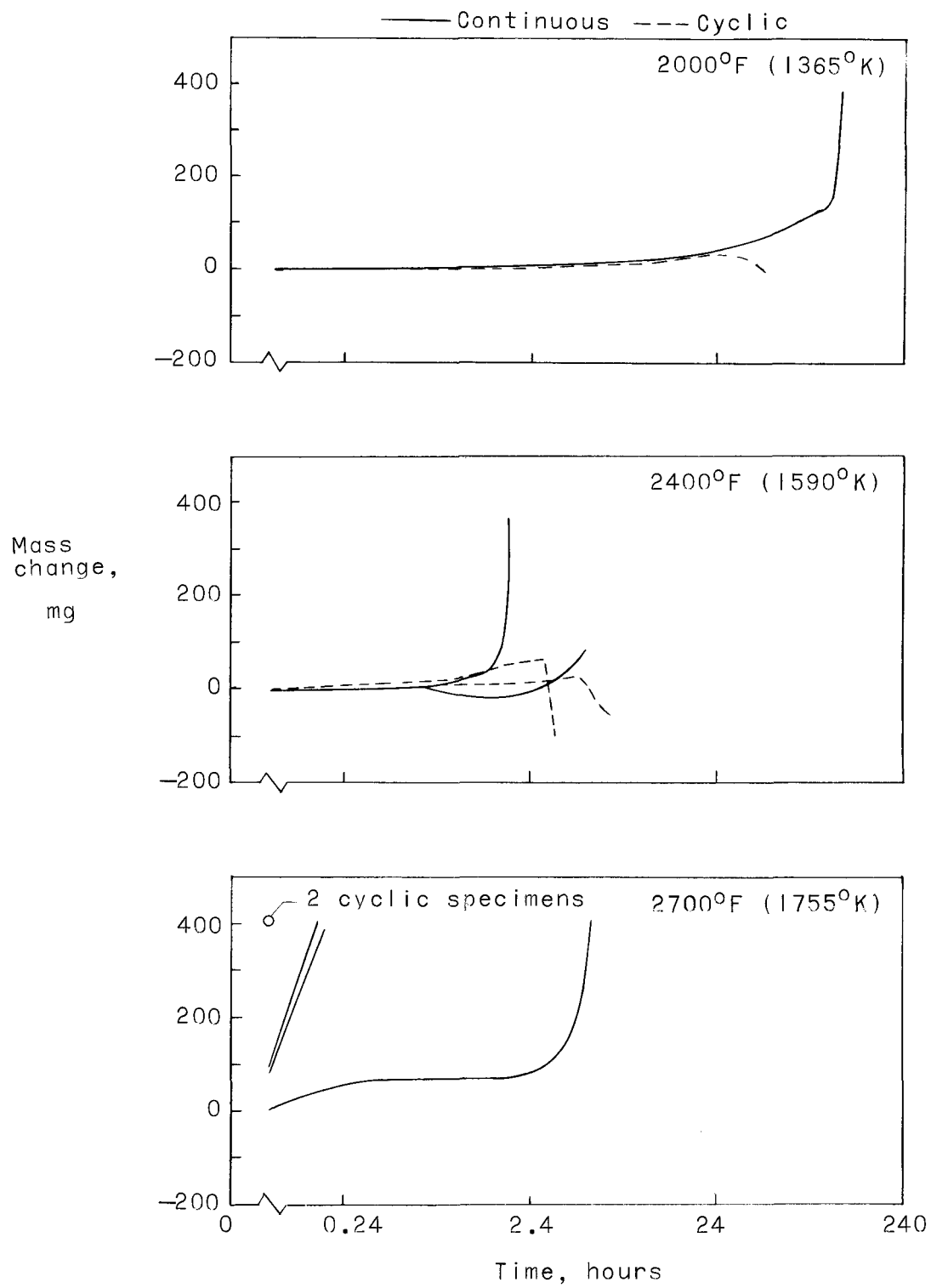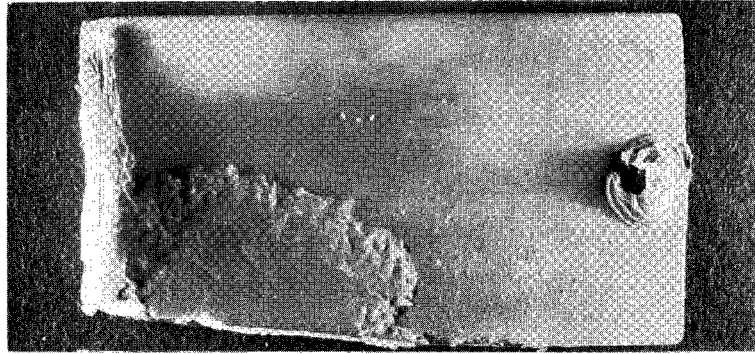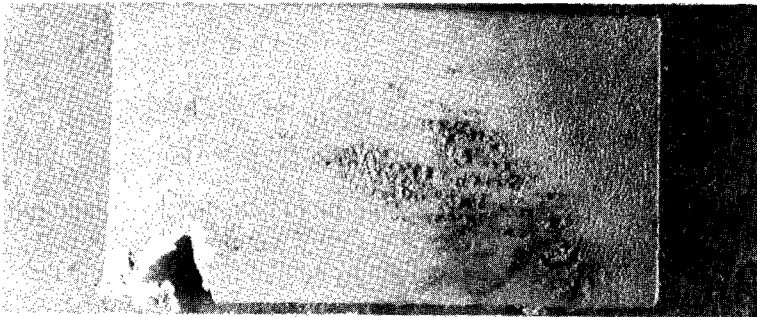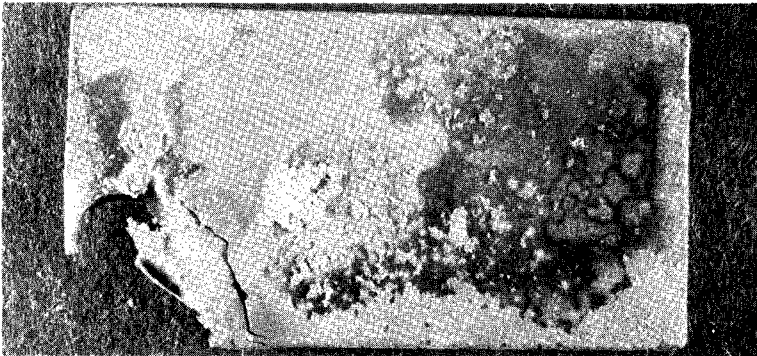Figure 2.- Appearance of coating 1 on Cb-10Ti-5Zr alloy sheet in the as-coated condition.
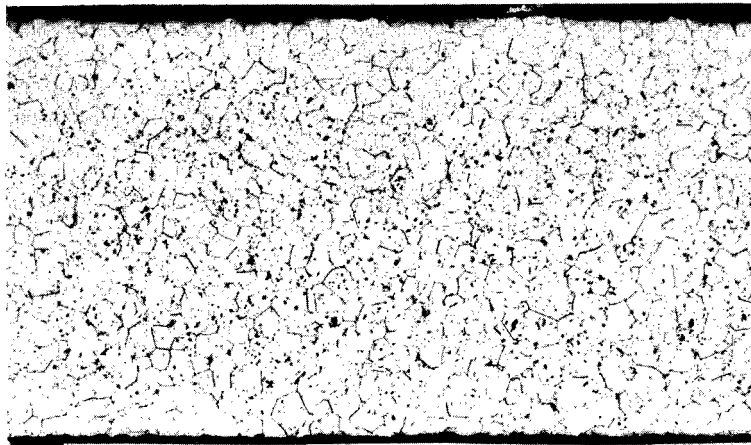
(a) Cross section, X 100.
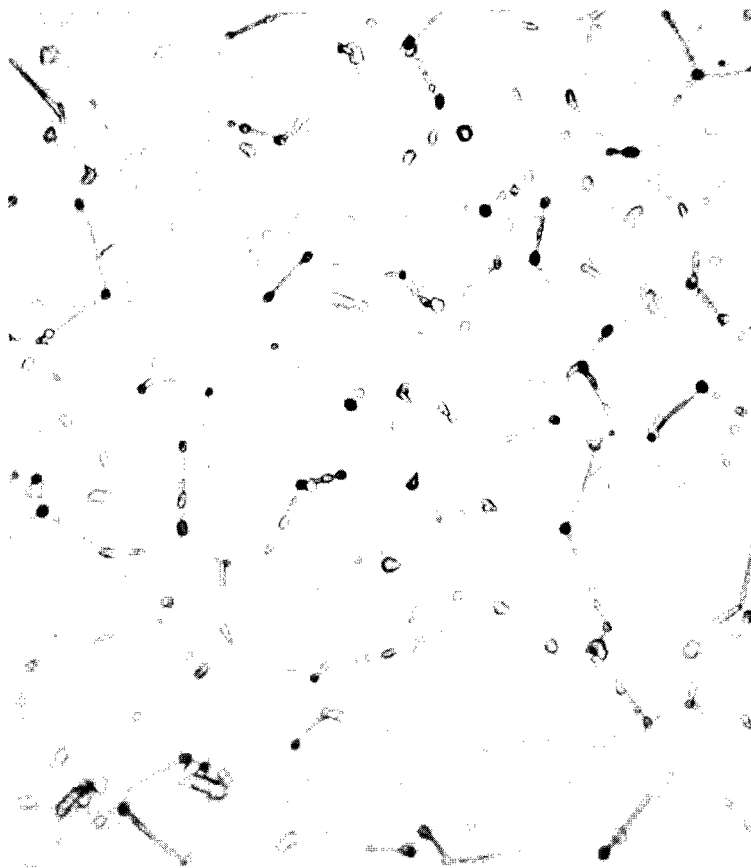
(b) Cross section, X 500.   L-65-7975

Figure 3.-   Photomicrographs of Cb-10Ti-5Zr alloy sheet in the annealed condition.
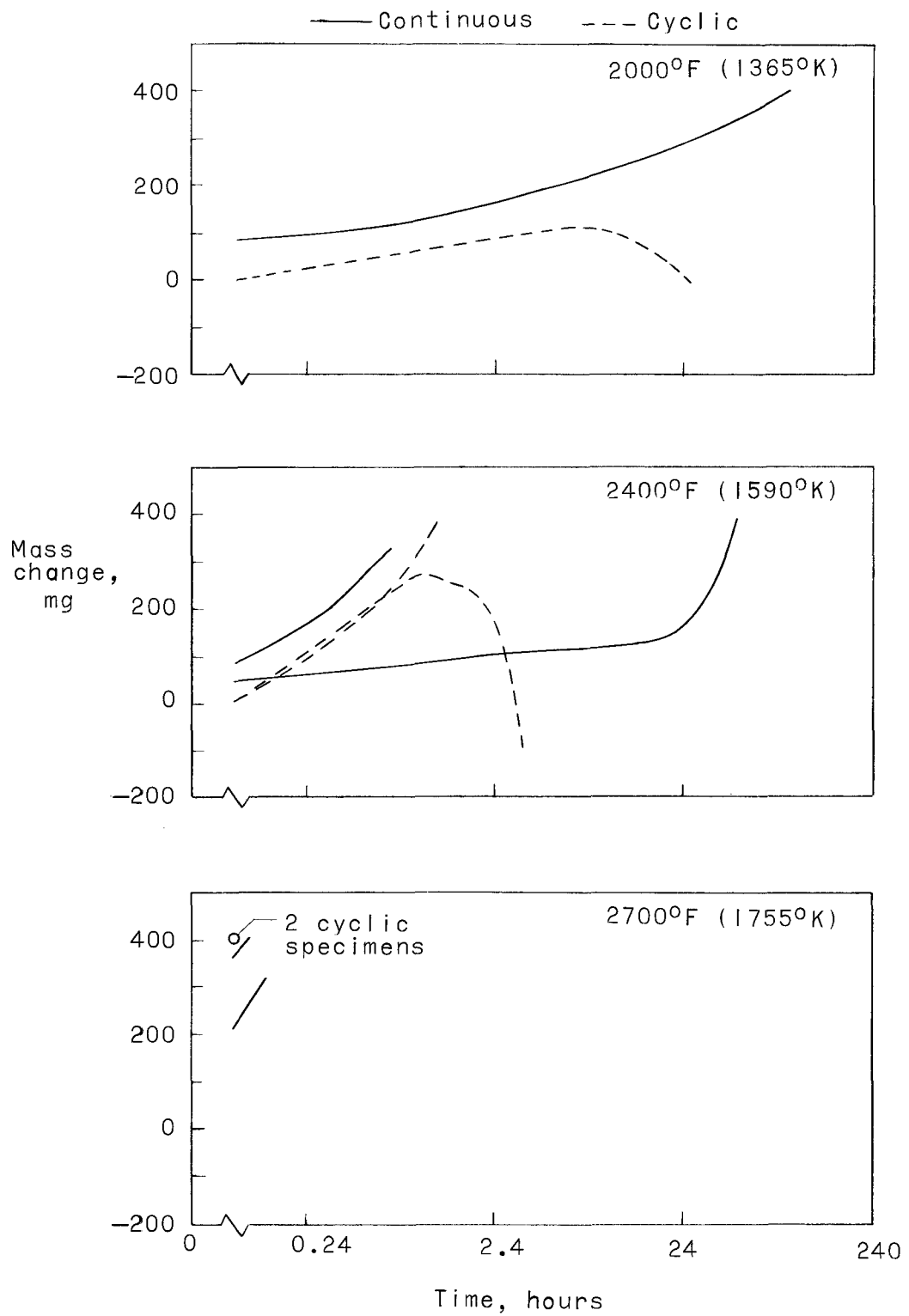
Figure 4.- Mass change histories for specimens of coating 1 on Cb-10Ti-5Zr alloy sheet tested in air at atmospheric pressure.

28
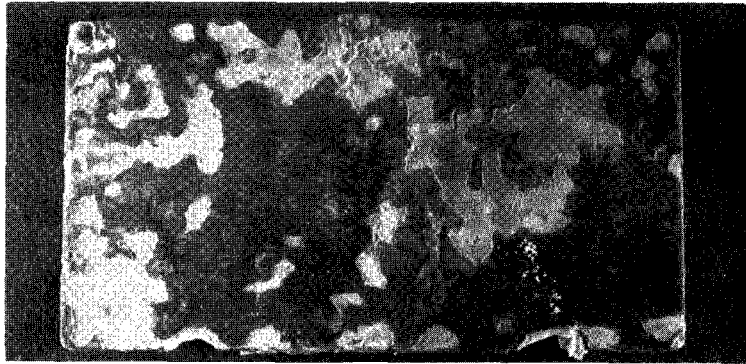
(a) 98-hour exposure at 2000⁰ F (1365⁰ K).

(b) 2-hour exposure at 2400⁰ F (1590⁰ K).
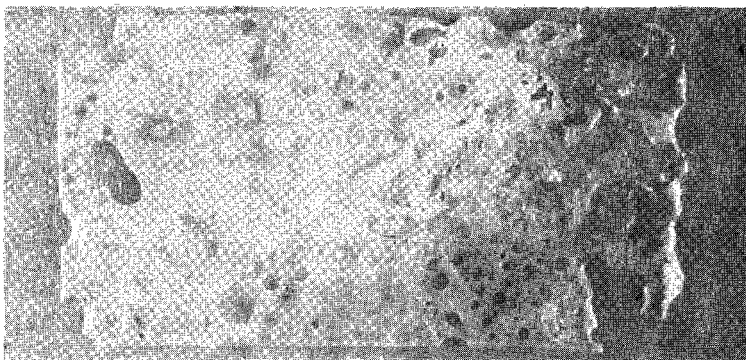
(c) 0.15-hour exposure at 2700⁰ F (1755⁰ K).   L-65-7976

Figure 5.- Photographs of tested specimens of coating 1 on Cb-10Ti-5Zr alloy sheet exposed in dry air at atmospheric pressure. X 2.
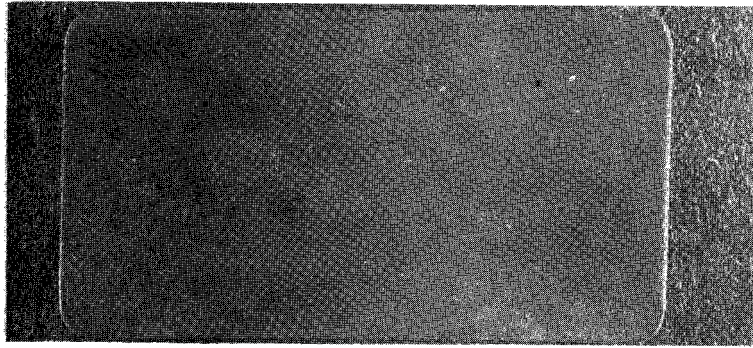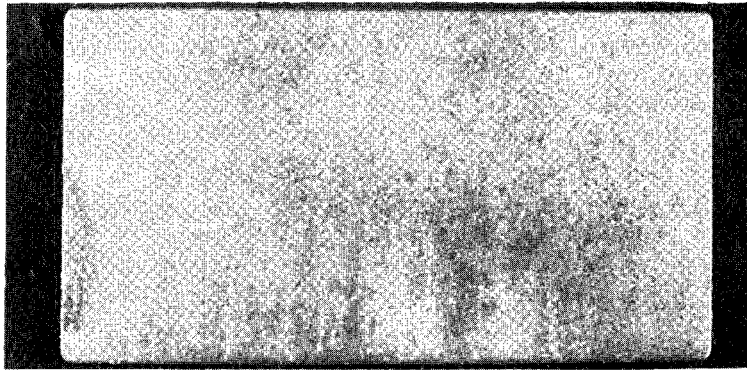
(a) As-coated appearance, X 2.
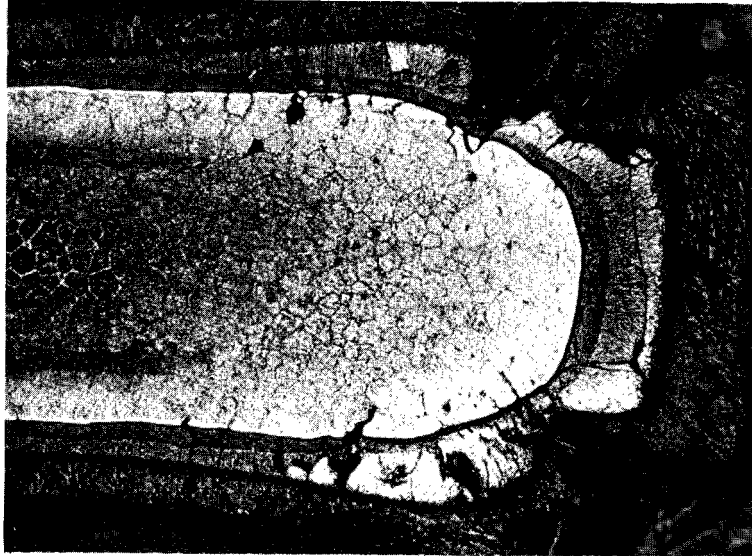
(b) Cross section, X 100.
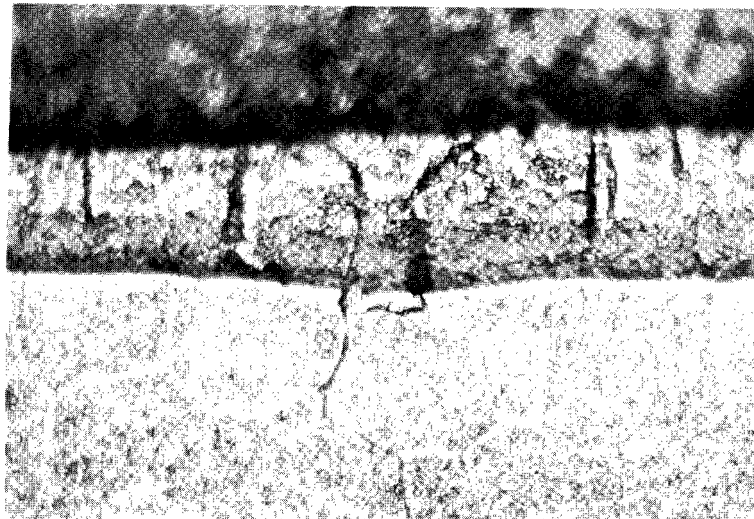
(c) Cross section, X 500.   L-65-7977

Figure 6.- Appearance of coating 2 on Cb-10Ti-5Zr alloy sheet in the as-coated condition.
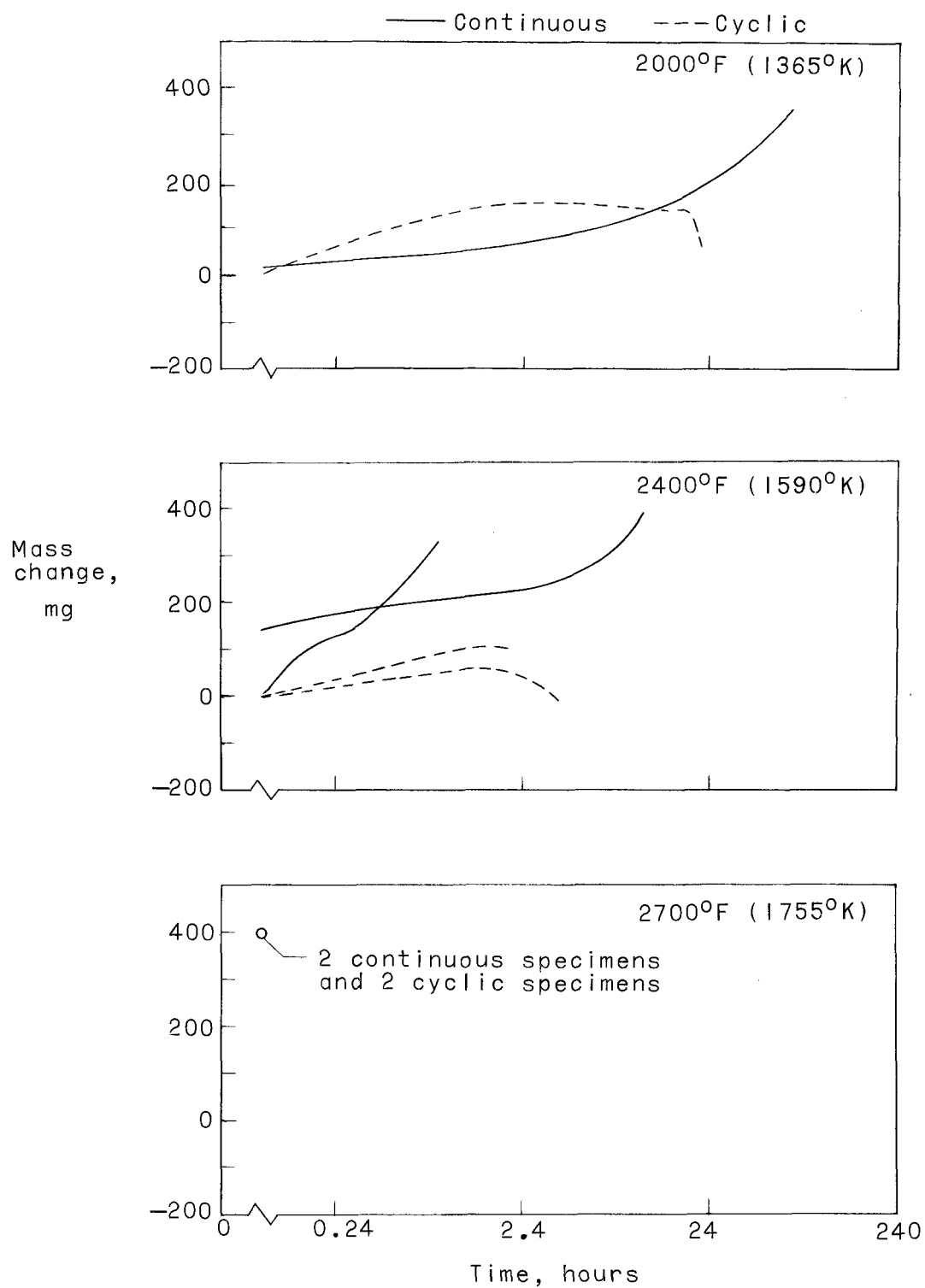
Figure 7.- Mass change histories for specimens of coating 2 on Cb-10Ti-5Zr alloy sheet tested in air at atmospheric pressure.
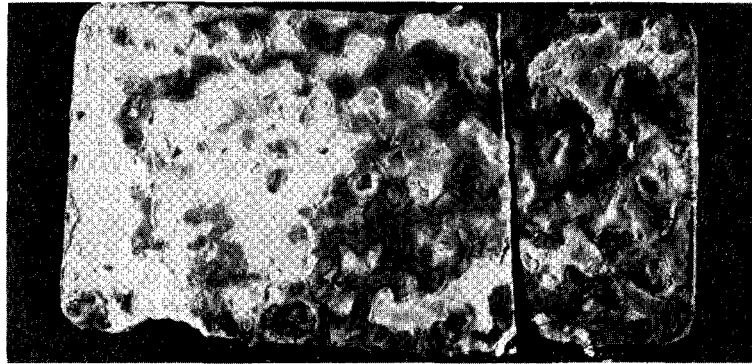
(a) 69-hour exposure at 2000° F (1365° K).
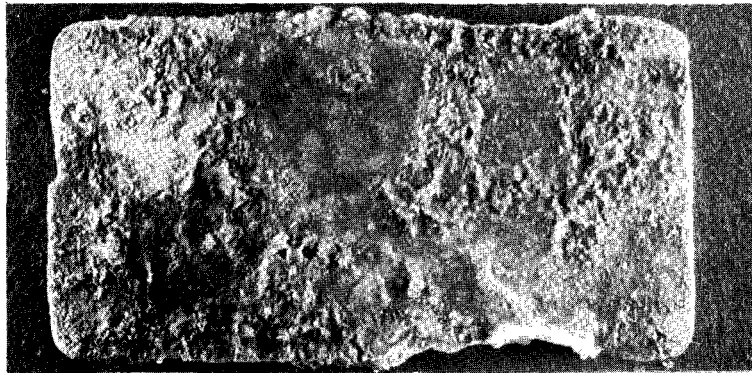
(b) 4-hour exposure at 2400° F (1590° K).

(c) 0.25-hour exposure at 2700° F (1755° K).   L-65-7978

Figure 8.-   Photographs of tested specimens of coating 2 on Cb-10Ti-5Zr alloy sheet exposed in air at atmospheric pressure,   X 2.
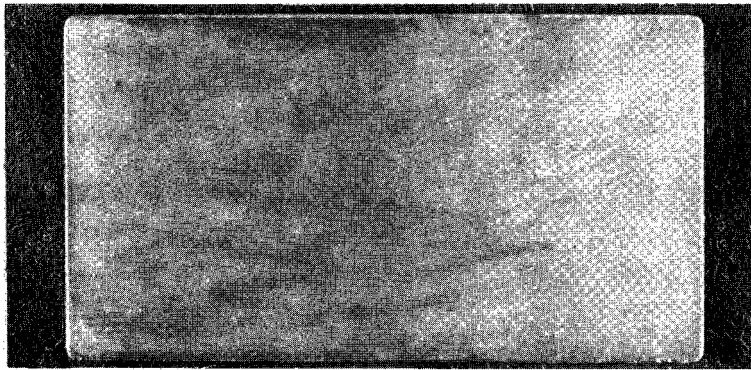
(a) As-coated appearance, X 2.

(b) Cross section, X 100.
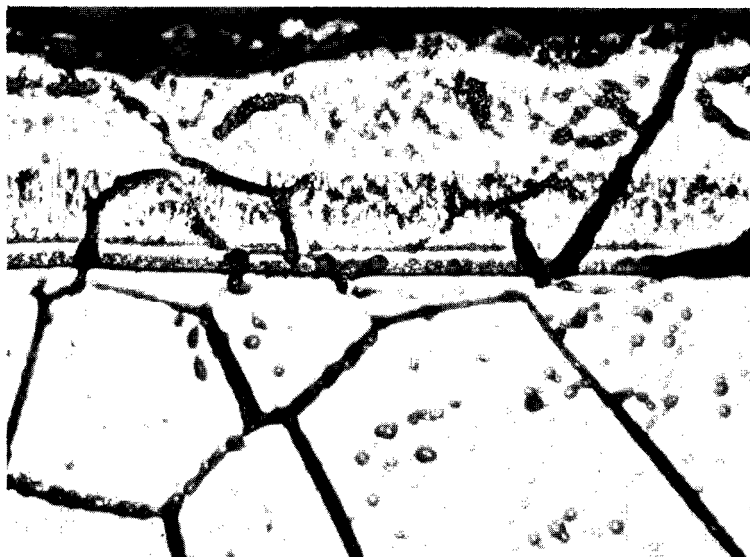
(c) Cross section, X 500.   L-65-7979

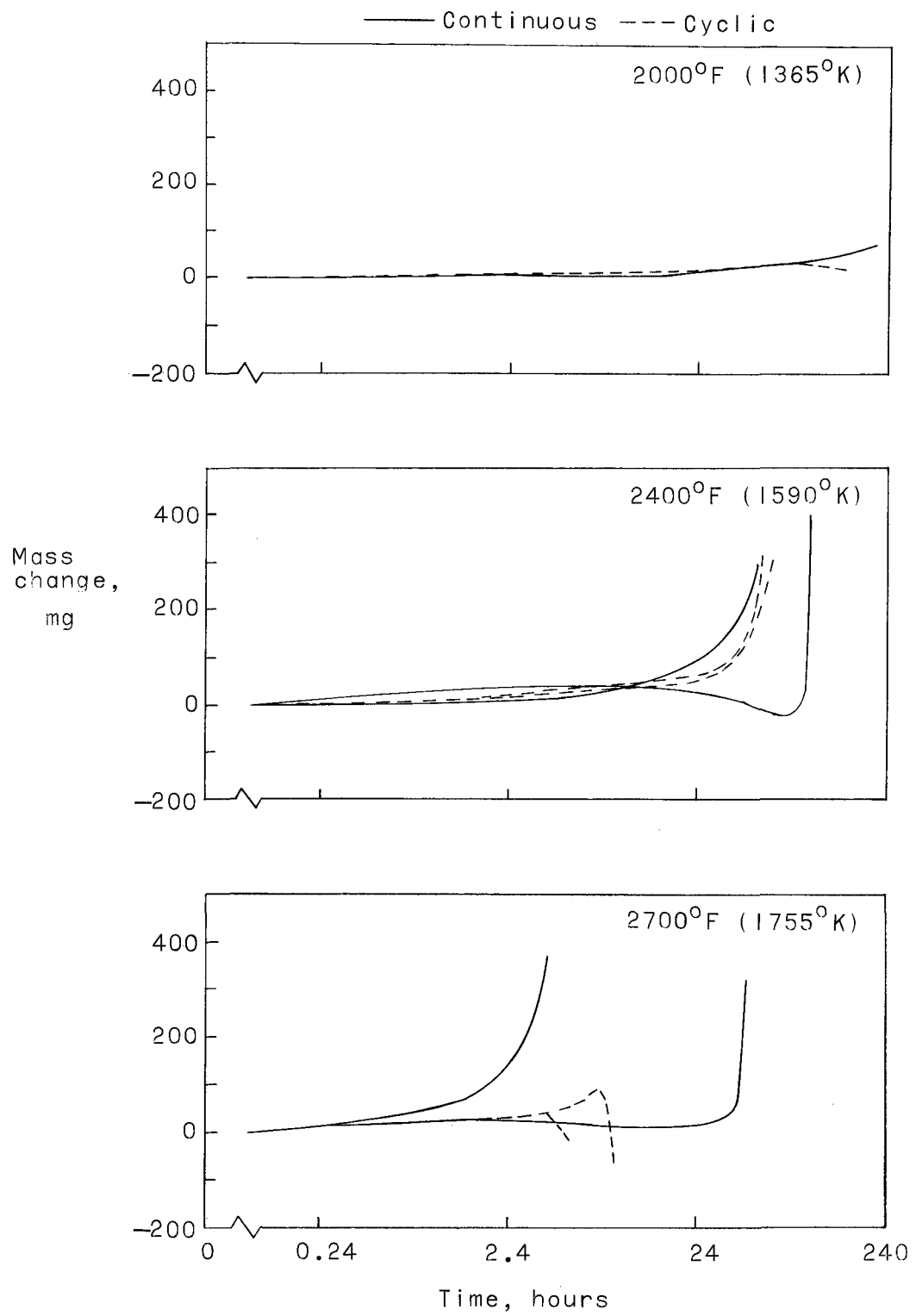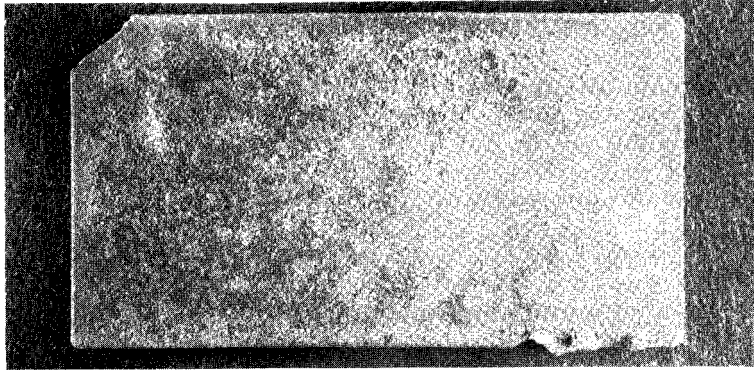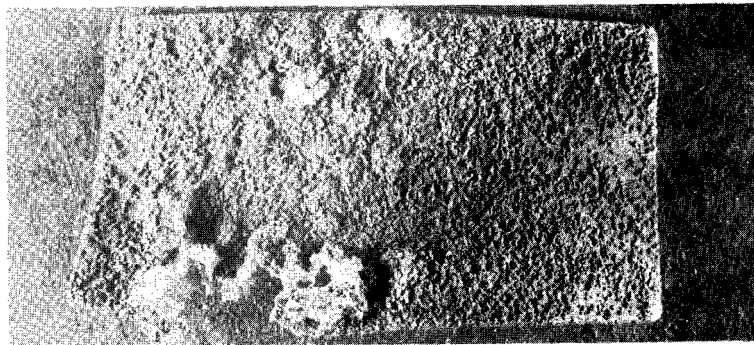Figure 9.- Appearance of coating 3 on Cb-10Ti-5Zr alloy sheet in the as-coated condition.
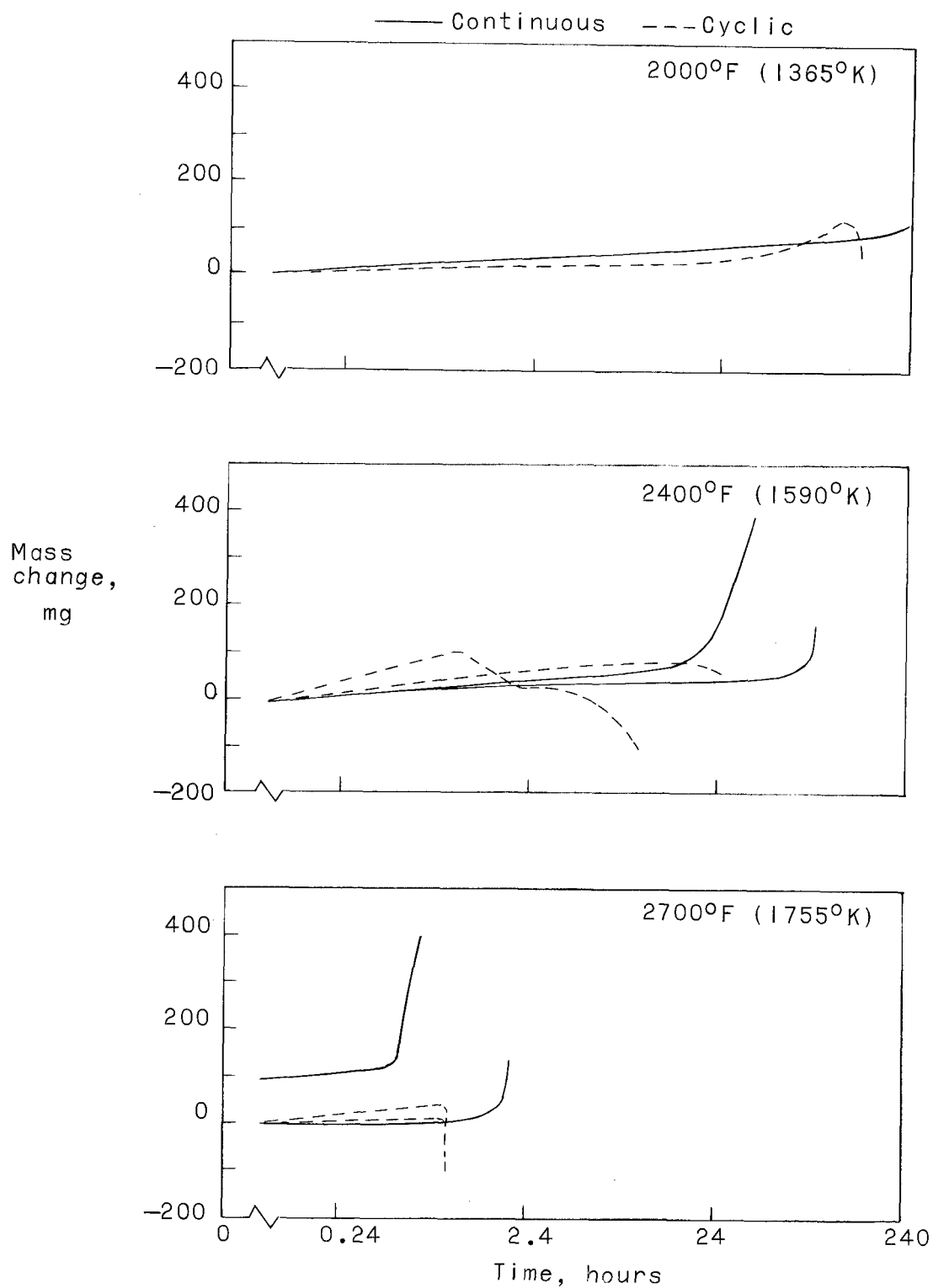
Figure 10.- Mass change histories for specimens of coating 3 on Cb-10Ti-5Zr alloy sheet tested in air at atmospheric pressure.
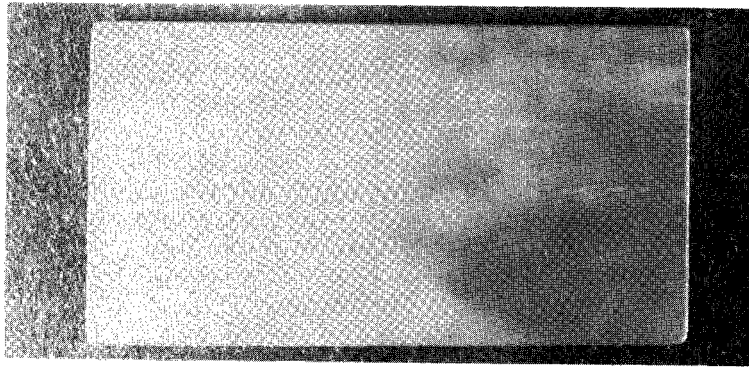
34
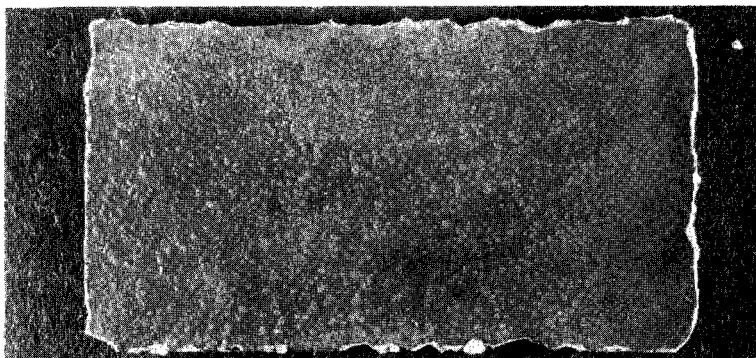
(a) 130-hour exposure at 2000° F (1365° K).
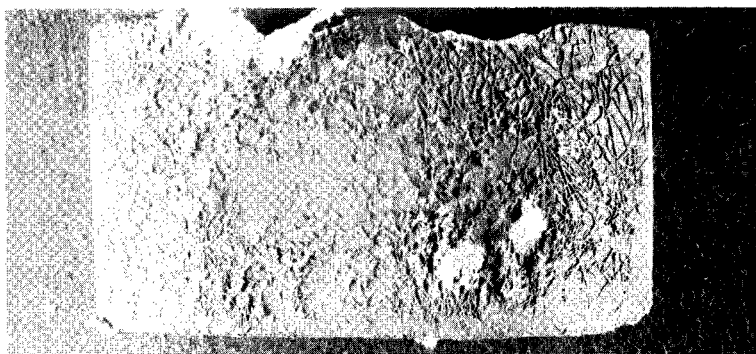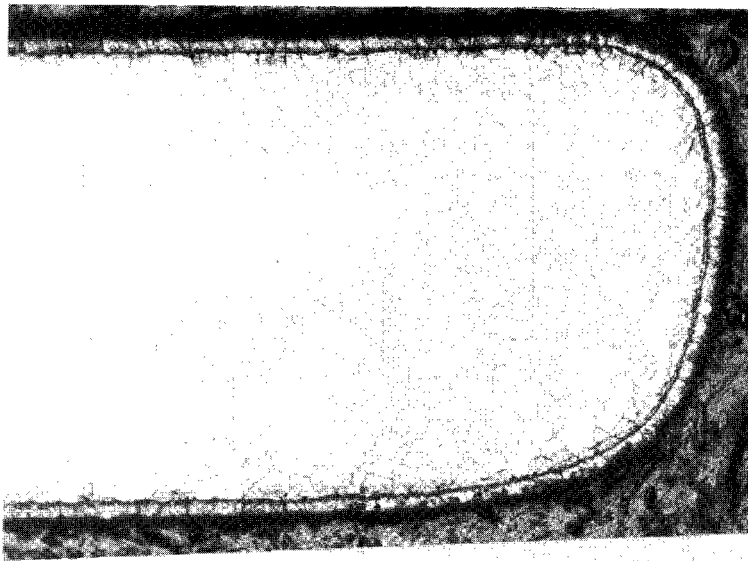

(b) 25-hour exposure at 2400° F (1590° K).

(c) 0.9-hour exposure at 2700° F (1755° K).   L-65-7980

Figure 11.- Photographs of tested specimens of coating 3 on Cb-10Ti-5Zr alloy sheet exposed in dry air at atmospheric pressure. X 2.
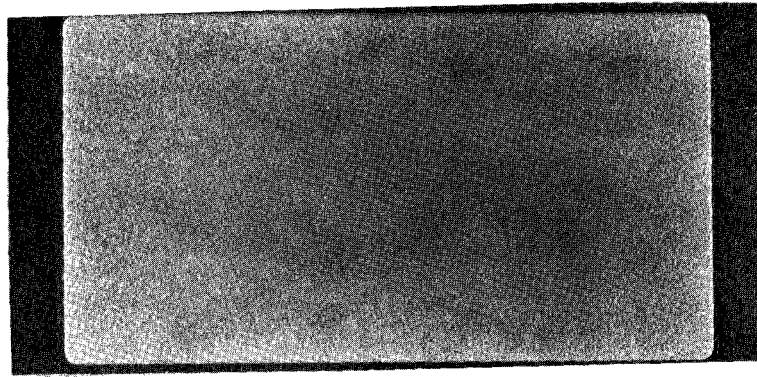
(a) As-coated appearance, X 2.

(b) Cross section, X 100.

(c) Cross section, X 500.   L-65-7981

Figure 12.- Appearance of coating 4 on Cb-10Ti-5Zr alloy sheet in the as-coated condition.
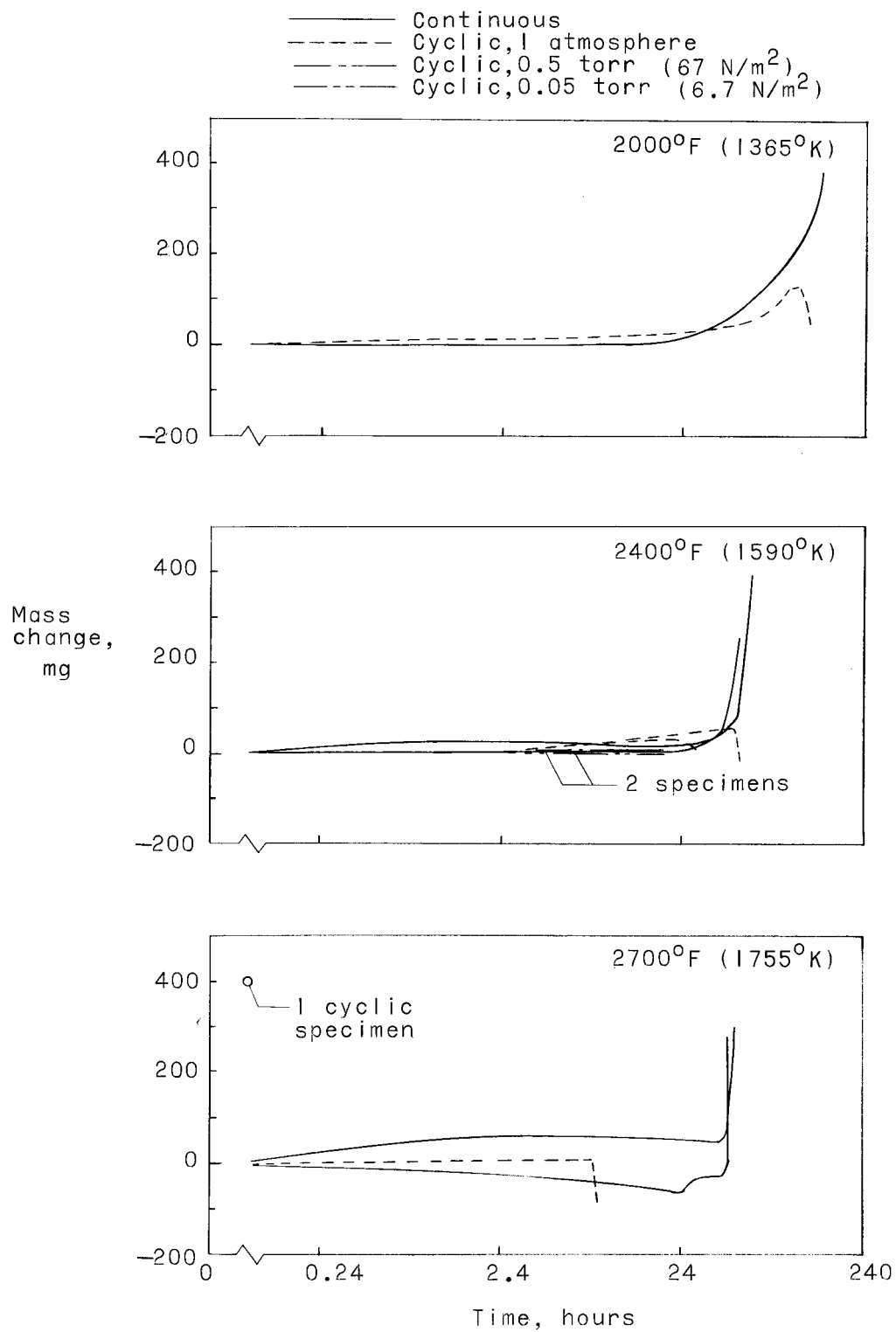
Figure 13.- Mass change histories for specimens of coating 4 on Cb-10Ti-5Zr alloy sheet tested in air.
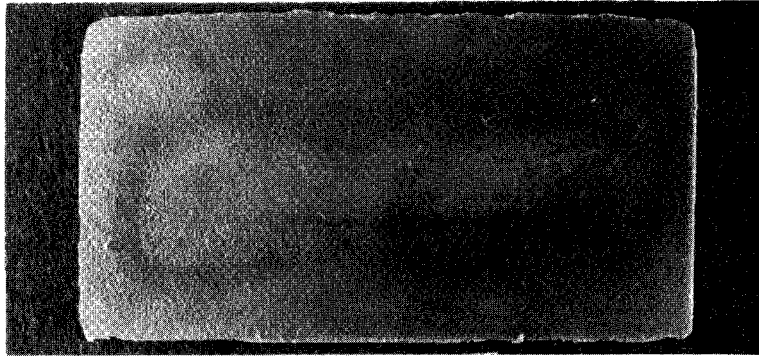
(a) 92-hour exposure at 2000° F (1365° K).
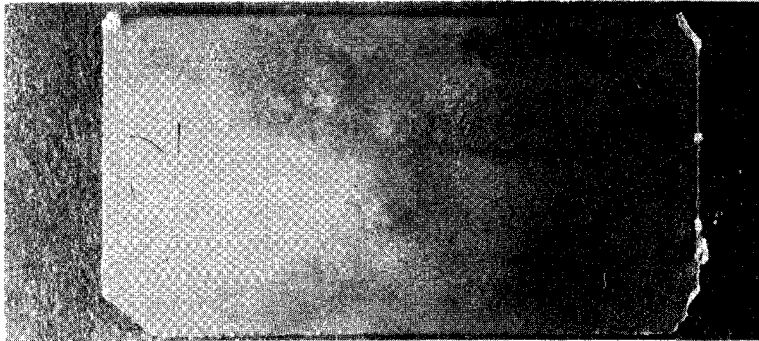
(b) 29-hour exposure at 2400° F (1590° K).
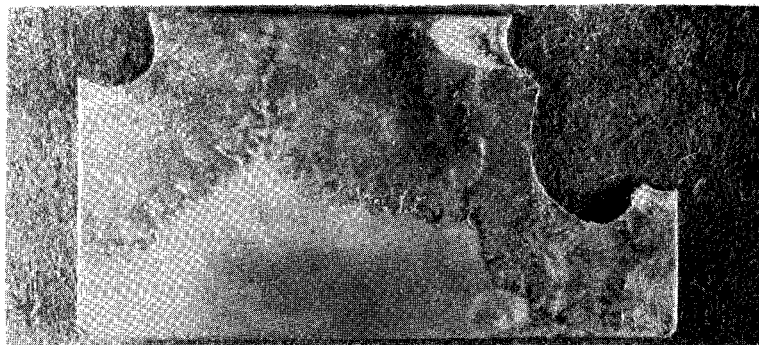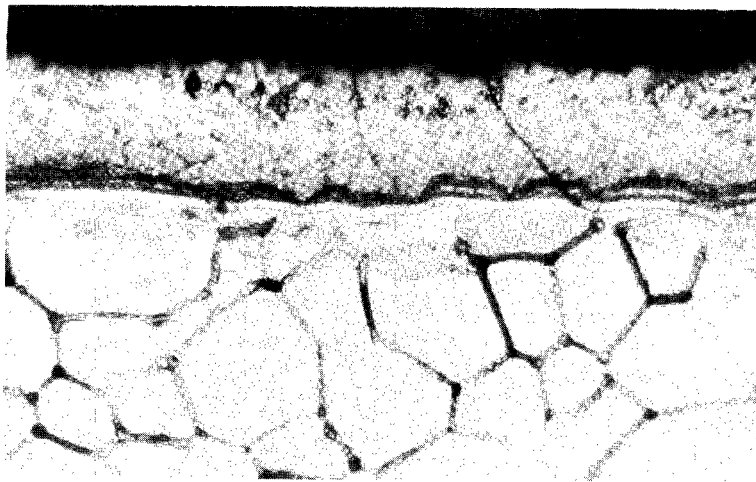

(c) 1-hour exposure at 2700° F (1755° K).   L-65-7982

Figure 14.- Photographs of tested specimens of coating 4 on Cb-10Ti-5Zr alloy sheet exposed in dry air at atmospheric pressure. X 2.
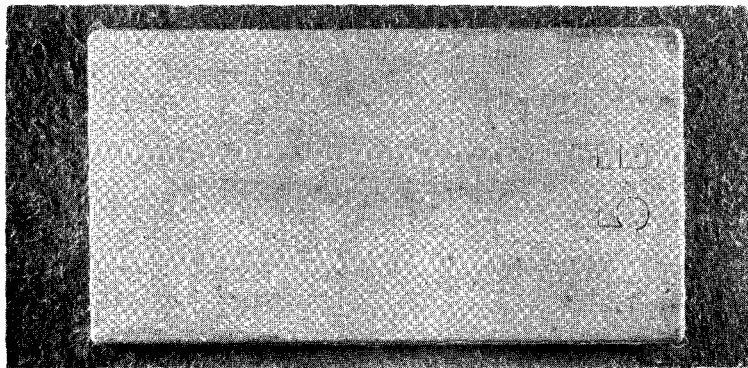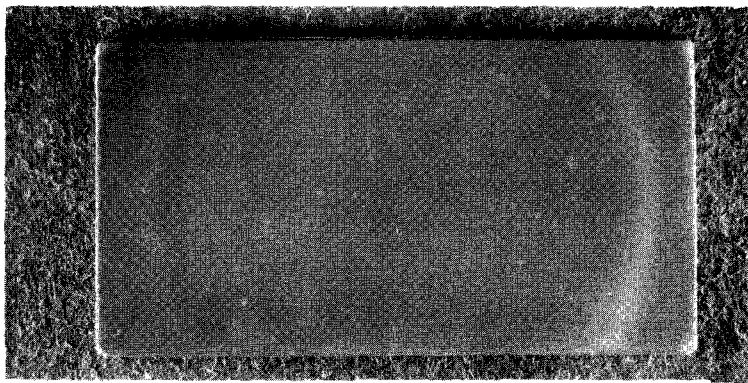
(a) 0.5 mm Hg $(66.7 \ N/m^2)$.

(b) 0.05 mm Hg $(6.67 \ N/m^2)$.   L-65-7983

Figure 15.- Appearance of tested specimens of coating 4 on Cb-10Ti-5Zr alloy sheet exposed for 20 one-hour cycles at 2400° F (1590° K) in air at reduced pressures. X 2.
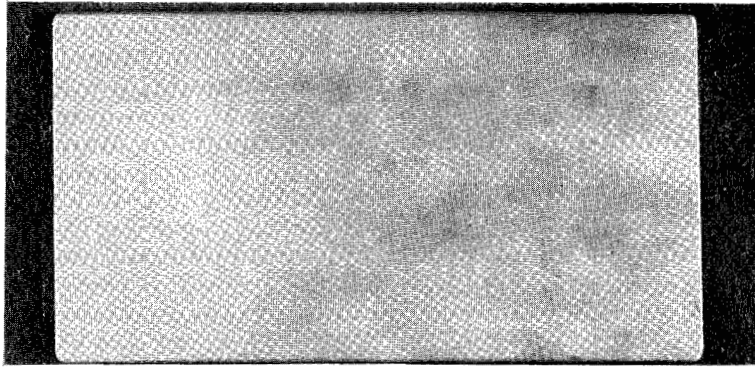
(a) As-coated appearance, X 2.
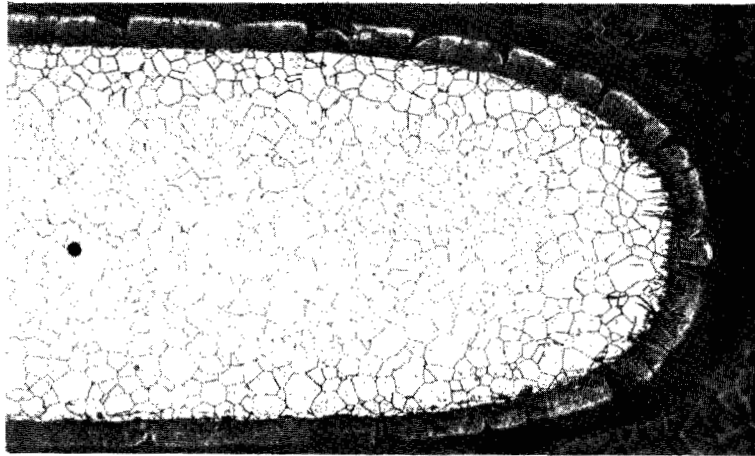
(b) Cross section, X 100.

SiC overcoat

(c) Cross section, X 500.   L-65-7984

Figure 16.- Appearance of coating 5 on Cb-10Ti-5Zr alloy sheet in the as-coated condition, showing SiC overcoat layer.
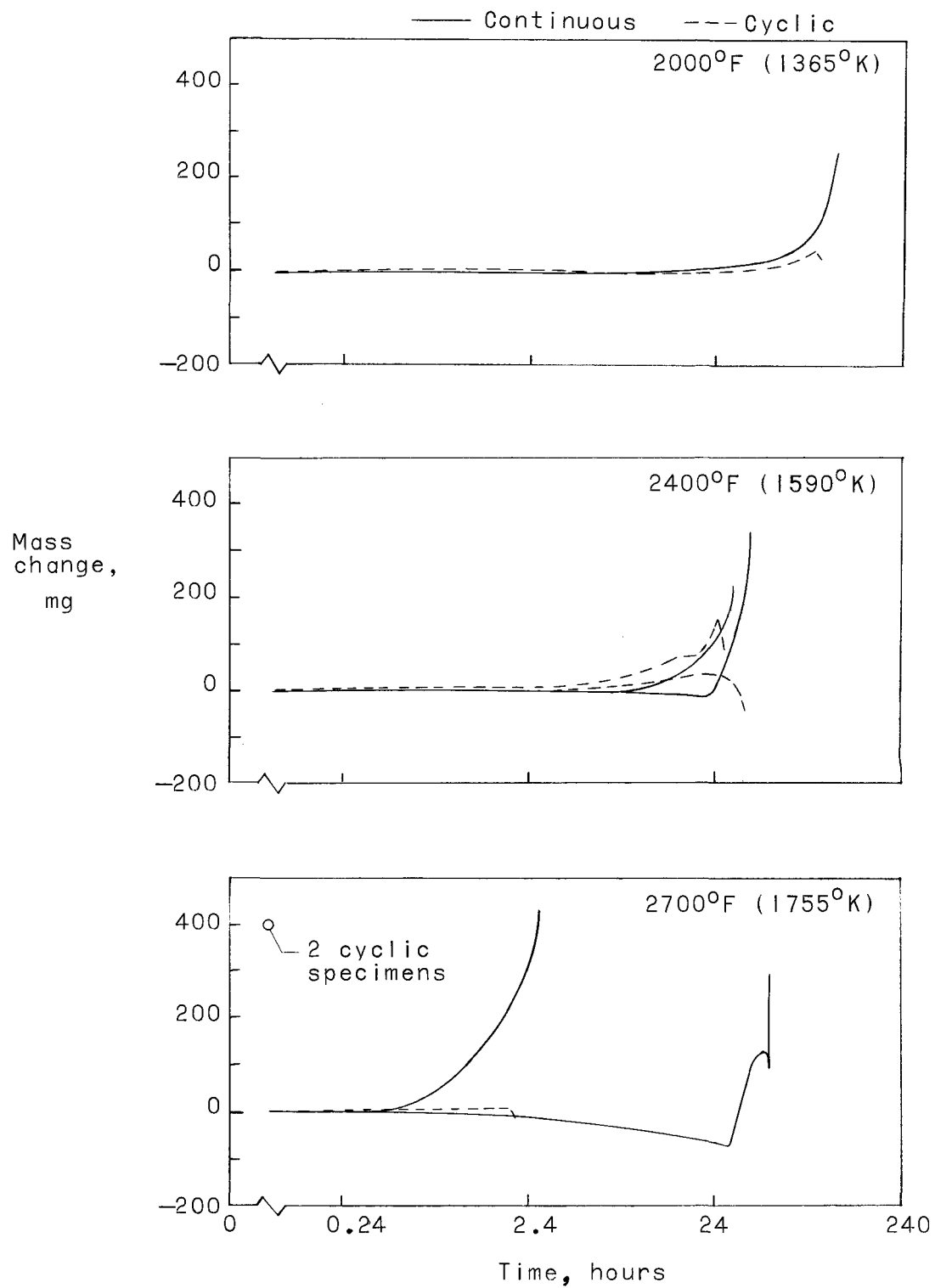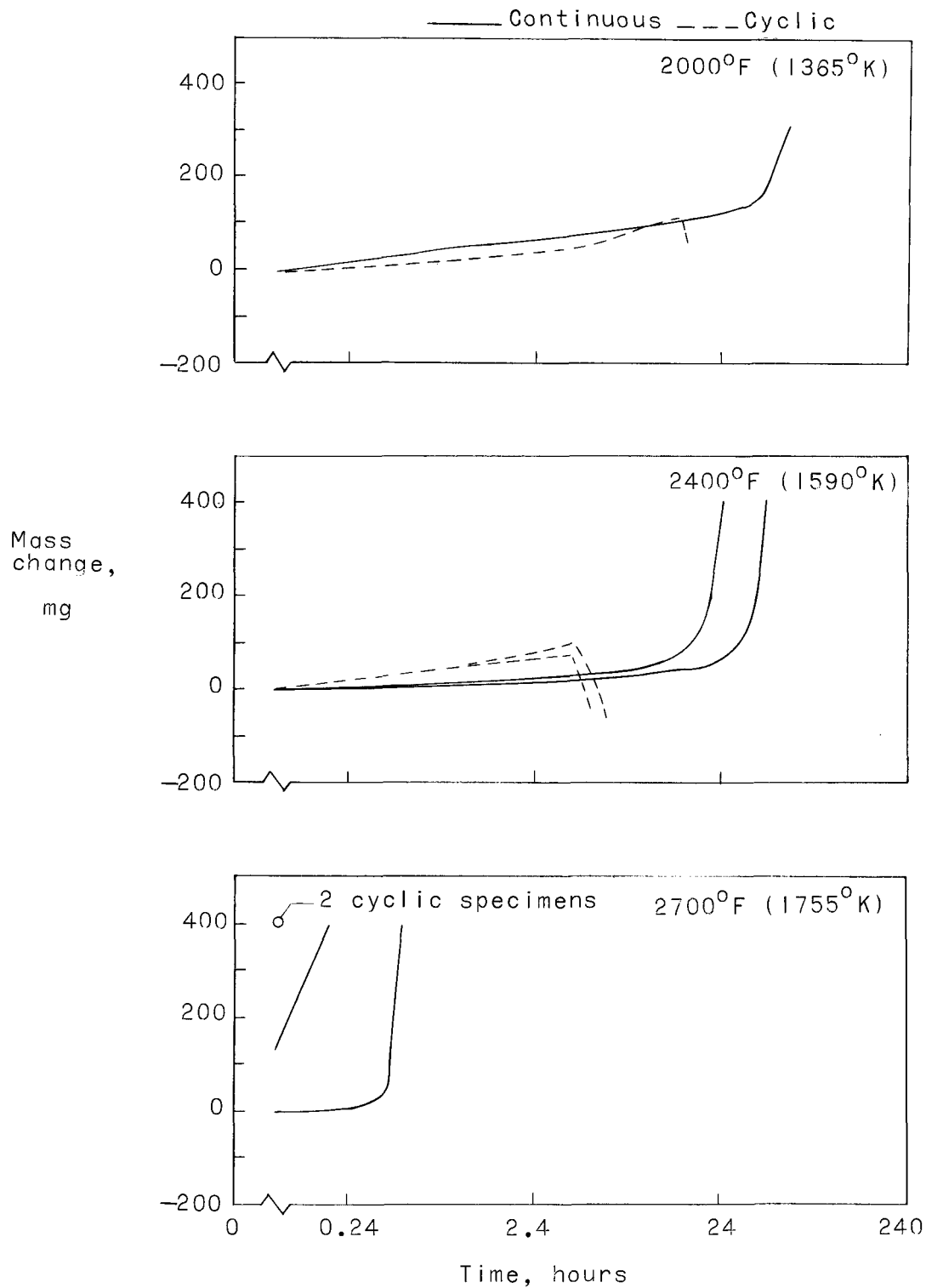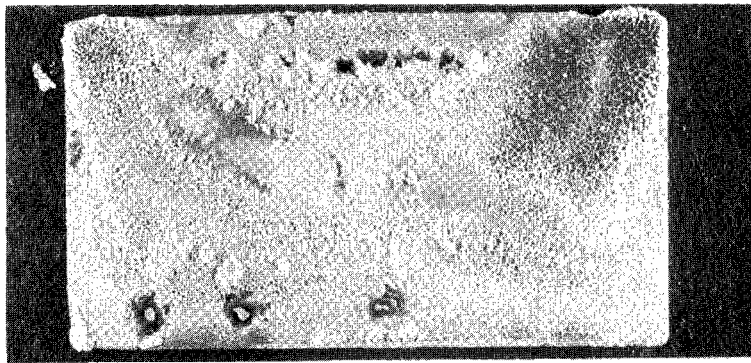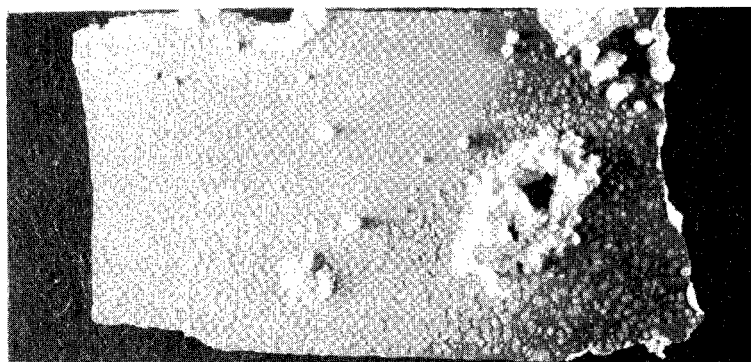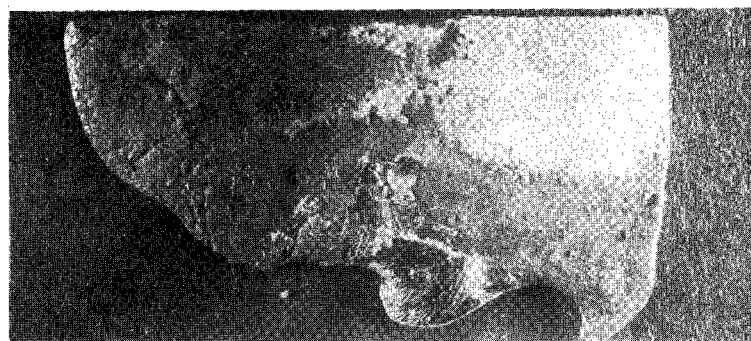
Figure 17.- Mass change histories for specimens of coating 5 on Cb-10Ti-5Zr alloy sheet tested in air at atmospheric pressure.

(a) 125-hour exposure at 2000° F (1365° K).

(b) 35-hour exposure at 2400° F (1590° K).
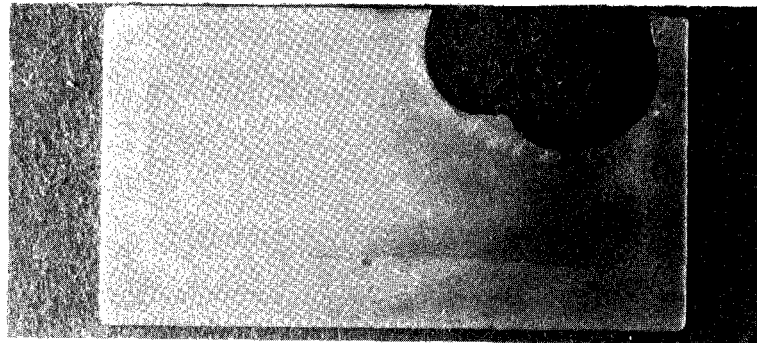
(c) 1-hour exposure at 2700° F (1755° K).   L-65-7985

Figure 18.- Photographs of tested specimens of coating 5 on Cb-10Ti-5Zr alloy sheet exposed in dry air at atmospheric pressure. X 2.
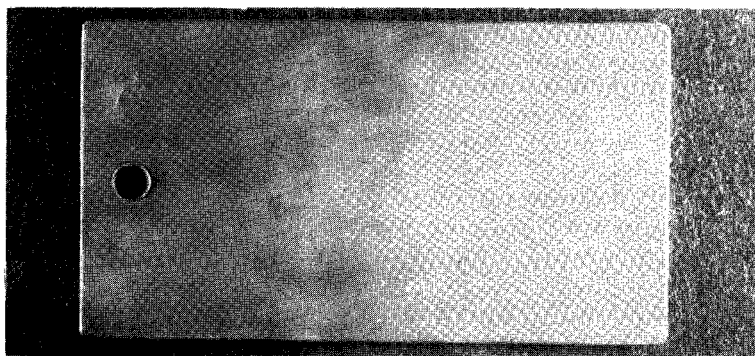
(a) As-coated appearance, X 2.
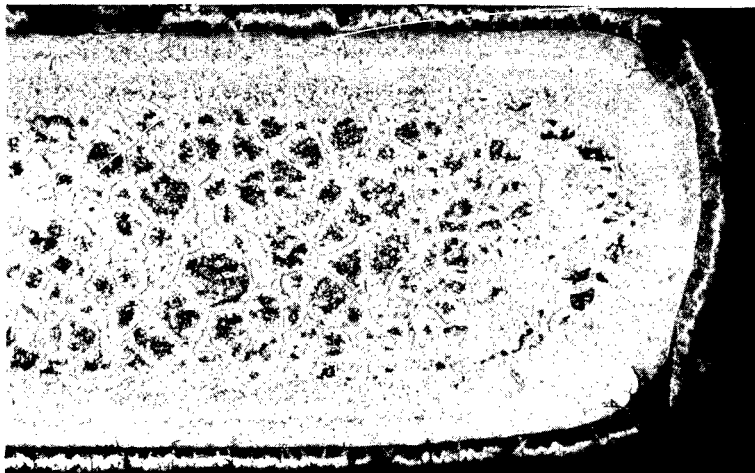
(b) Cross section, X 100.

(c) Cross section, X 500.   L-65-7986

Figure 19.- Appearance of coating 6 on Cb-10Ti-5Zr alloy sheet in the as-coated condition.

Figure 20.- Mass change histories for specimens of coating 6 on Cb-10Ti-5Zr alloy sheet tested in air at atmospheric pressure.

44

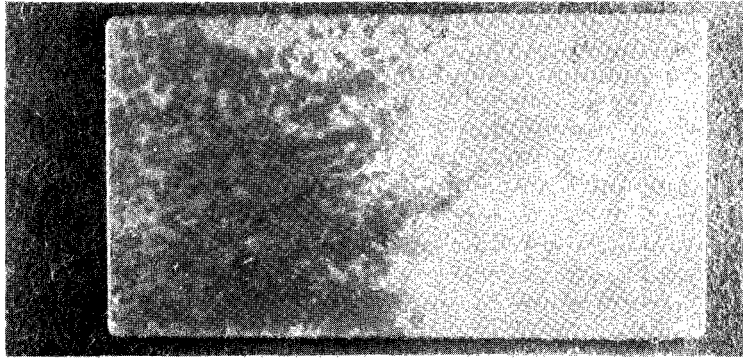(a) 144-hour exposure at 2000° F (1365° K).
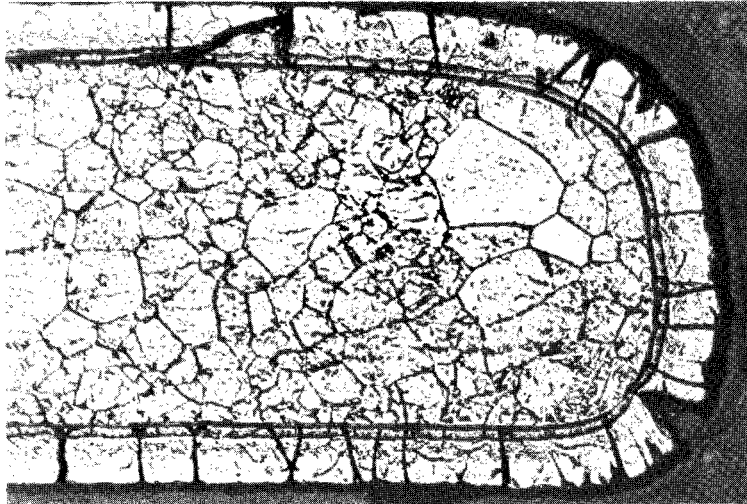

(b) 75-hour exposure at 2400° F (1590° K).

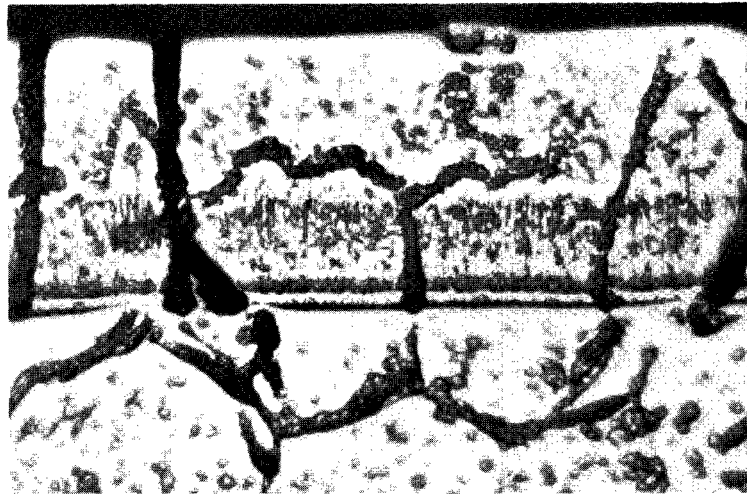(c) 1.4-hour exposure at 2700° F (1755° K).   L-65-7987

Figure 21.- Photographs of tested specimens of coating 6 on Cb-10Ti-5Zr alloy sheet exposed in dry air at atmospheric pressure under the conditions noted. X 2.

45
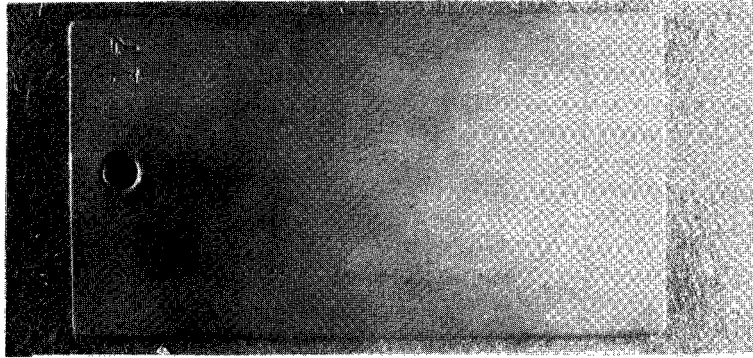
(a) As-coated appearance, X 2.
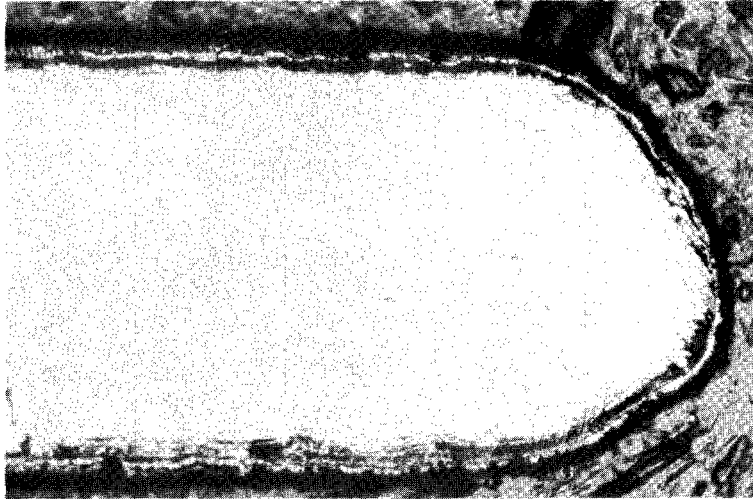
(b) Cross section, X 100.
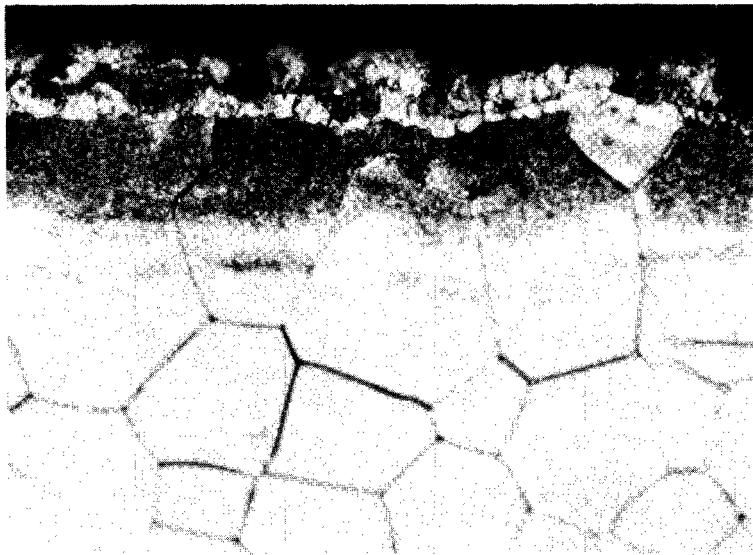
(c) Cross section, X 500.   L-65-7988

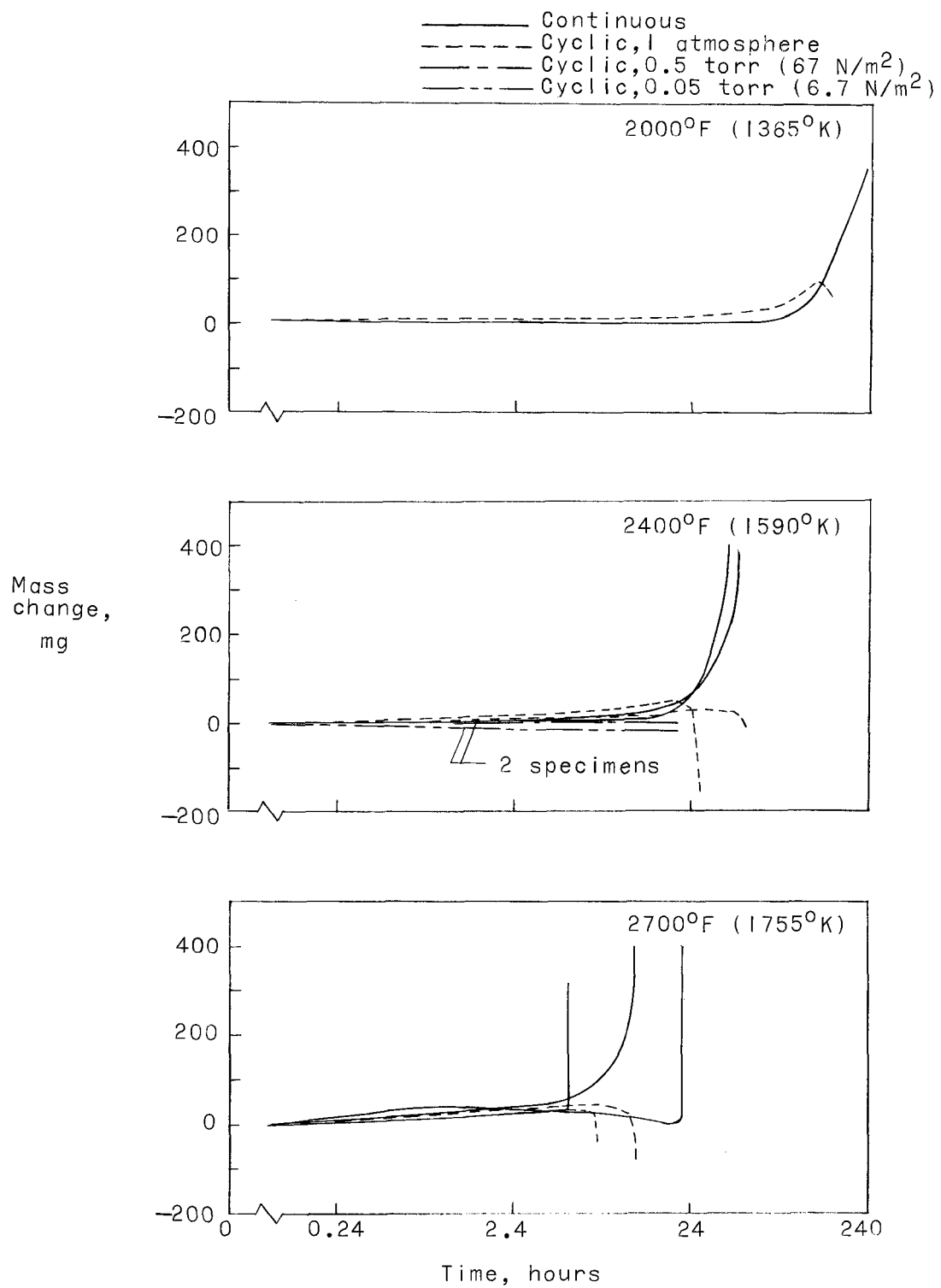Figure 22.- Appearance of coating 7 on Cb-10Ti-5Zr alloy sheet in the as-coated condition.

46

Figure 23.- Mass change histories for specimens of coating 7 on Cb-10Ti-5Zr alloy sheet tested in air at atmospheric pressure.

(a) 113-hour exposure at 2000° F (1365° K).

(b) 5-hour exposure at 2400° F (1590° K).

(c) 0.5-hour exposure at 2700° F (1755° K).   L-65-7989

Figure 24.- Photographs of tested specimens of coating 7 on Cb-10Ti-5Zr alloy sheet exposed in dry air at atmospheric pressure. X 2.
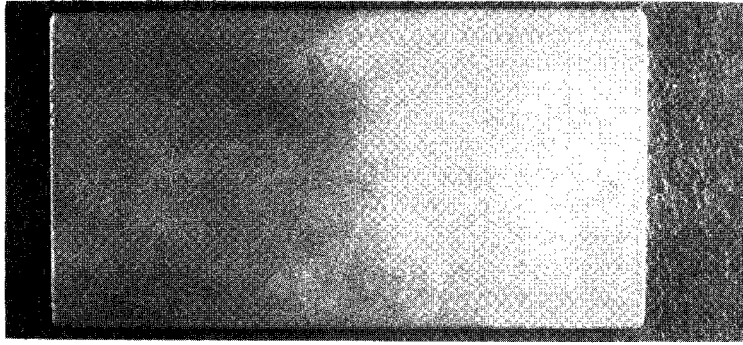
(a) As-coated appearance, X 2.
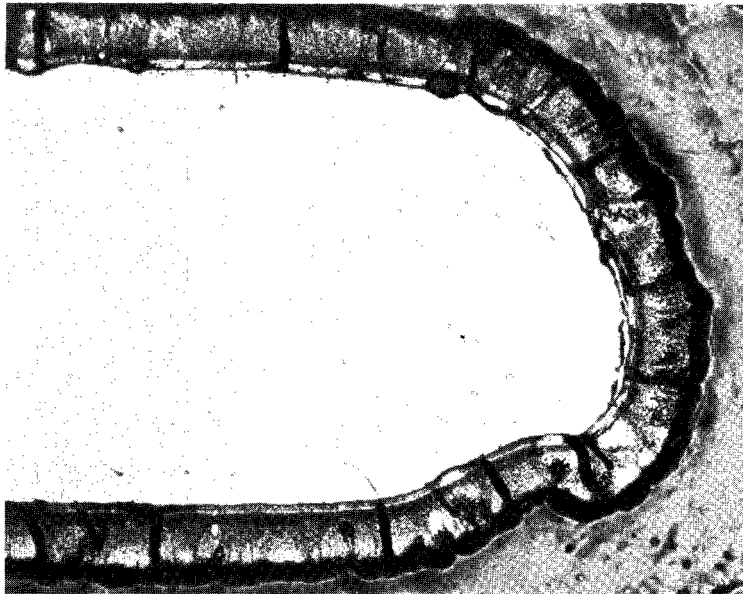
(b) Cross section, X 100.
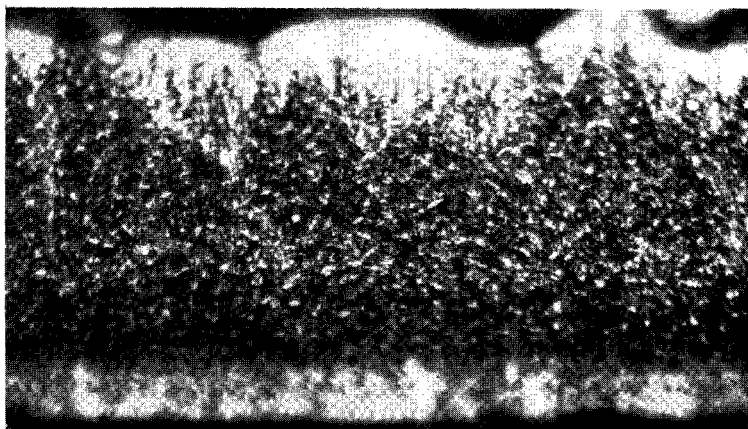
(c) Cross section, X 500.   L-65-7990

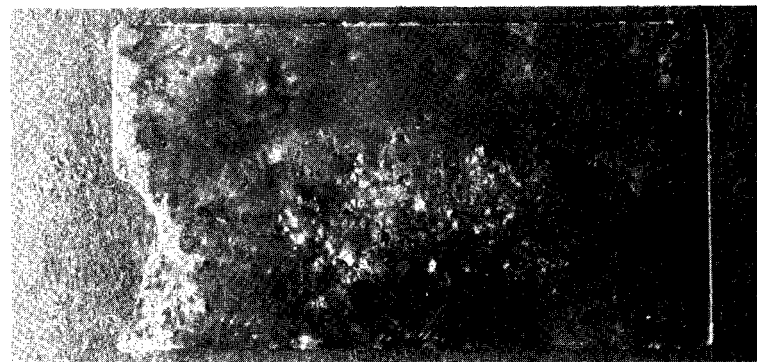Figure 25.- Appearance of coating 8 on Cb-10Ti-5Zr alloy sheet in the as-coated condition.

49
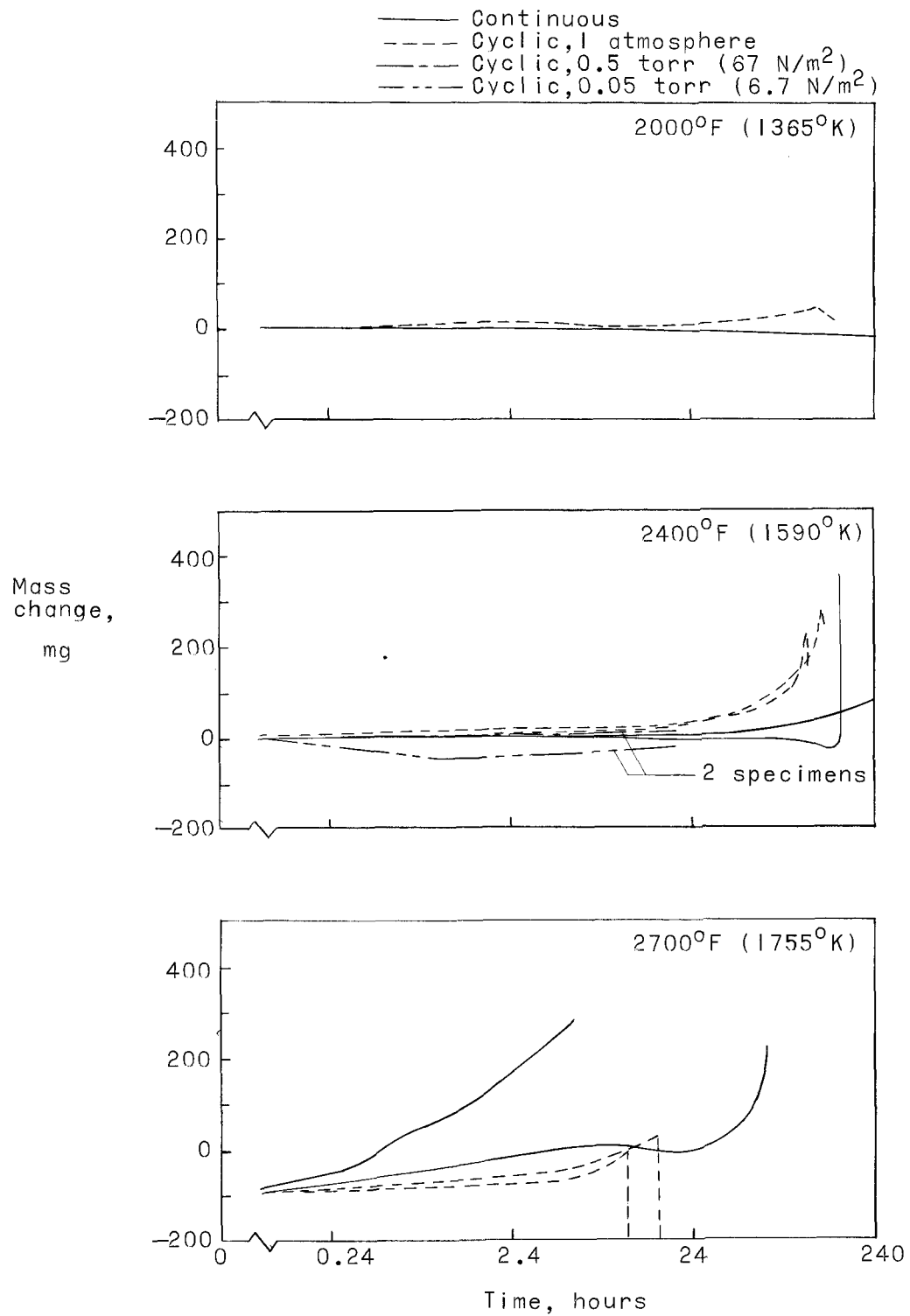
Figure 26.- Mass change histories for specimens of coating 8 on Cb-10Ti-5Zr alloy sheet tested in air.
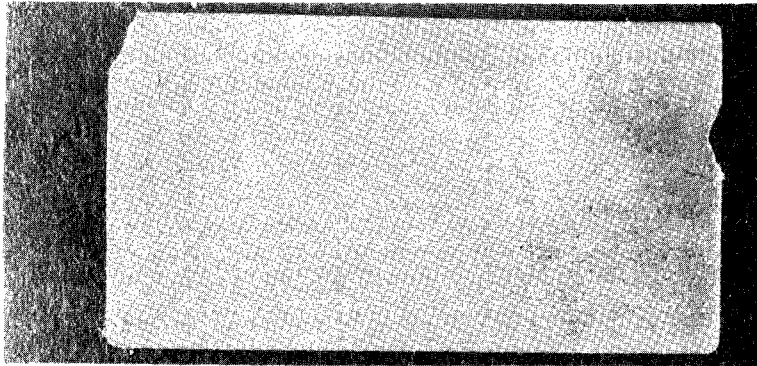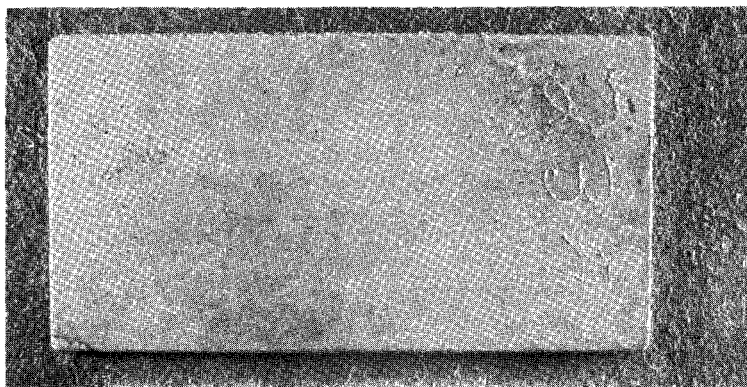
(a) 140-hour exposure at 2000° F (1365° K).

(b) 105-hour exposure at 2400° F (1590° K).

(c) 6-hour exposure at 2700° F (1755° K).   L-65-7991

Figure 27.- Photographs of tested specimens of coating 8 on Cb-10Ti-5Zr alloy sheet exposed in dry air at atmospheric pressure. X 2.
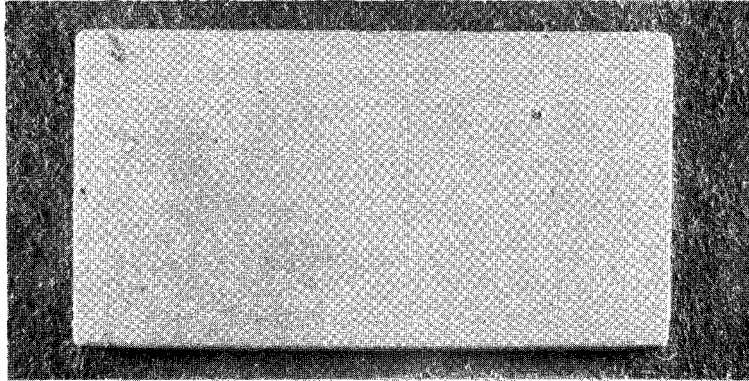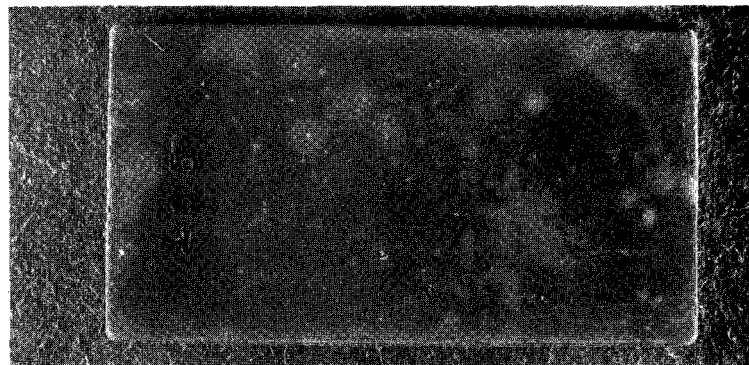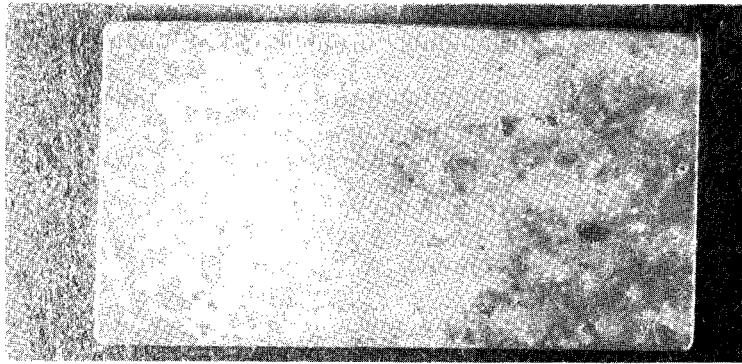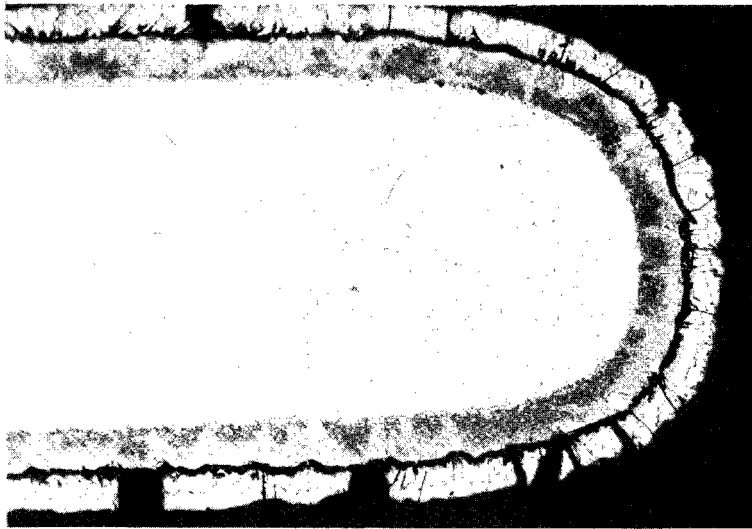
(a) 0.5 mm Hg $(66.7$ N/m$^2)$.

(b) 0.05 mm Hg $(6.67$ N/m$^2)$.   L-65-7992

Figure 28.- Appearance of tested specimens of coating 8 on Cb-10Ti-5Zr alloy sheet exposed for 20 one-hour cycles at 2400° F (1590° K) in air at reduced pressures. X 2.

(a) As-coated appearance, X 2.

(b) Cross section, X 100.

(c) Cross section, X 500.   L-65-7993

Figure 29.- Appearance of coating 9 on Cb-10Ti-5Zr alloy sheet in the as-coated condition.

Figure 30.- Mass change histories for specimens of coating 9 on Cb-10Ti-5Zr alloy sheet tested in air at atmospheric pressure.

(a) 143-hour exposure at 2000° F (1365° K).

(b) 53-hour exposure at 2400° F (1590° K).

(c) 4-hour exposure at 2700° F (1455° K).   L-65-7994

Figure 31.- Photographs of tested specimens of coating 9 on Cb-10Ti-5Zr alloy sheet exposed in dry air at atmospheric pressure. X 2.

(a) As-coated appearance, X 2.

(b) Cross section, X 100.

(c) Cross section, X 500.   L-65-7995

Figure 32.- Appearance of coating 10 on Cb-10Ti-5Zr alloy sheet in the as-coated condition.
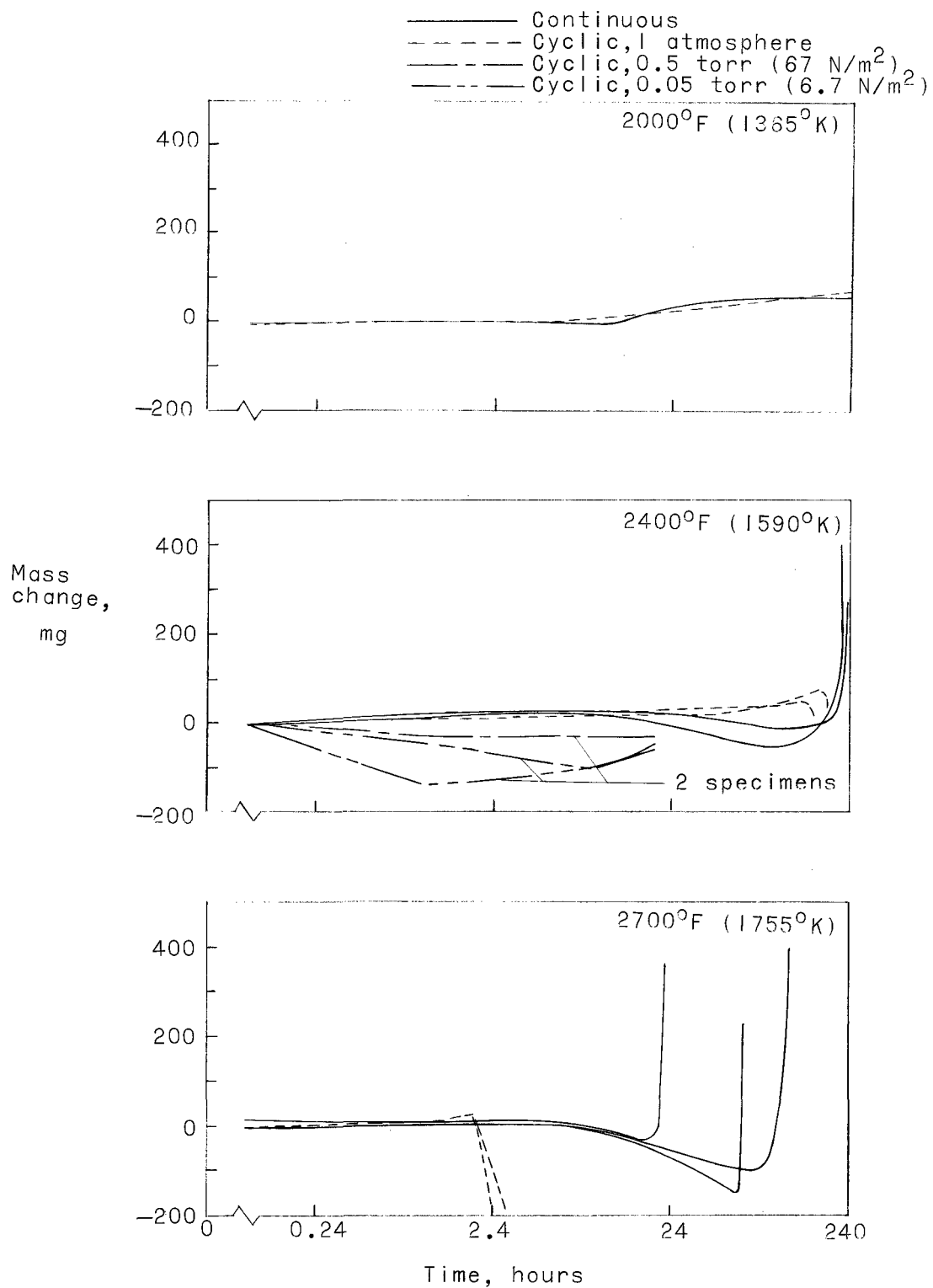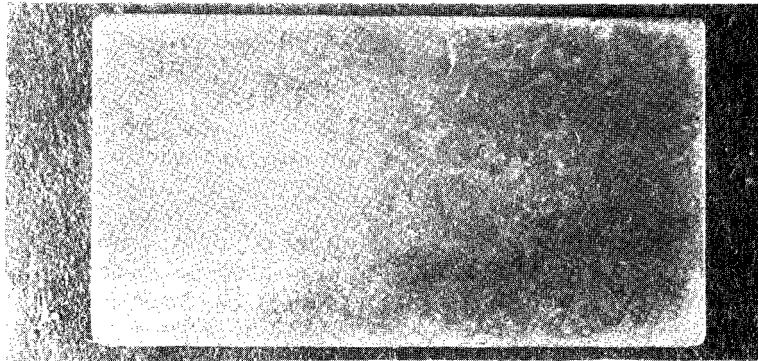
Figure 33.- Mass change histories for specimens of coating 10 on Cb-10Ti-5Zr alloy sheet tested in air at atmospheric pressure.

(a) 16-hour exposure at 2000° F (1365° K).

(b) 46-hour exposure at 2400° F (1590° K).

(c) 0.2-hour exposure at 2700° F (1755° K).   L-65-7996

Figure 34.-   Photographs of tested specimens of coating 10 on Cb-10Ti-5Zr alloy sheet exposed in dry air at atmospheric pressure.   X 2.

(a) As-coated appearance, X 2.

(b) Cross section, X 100.

(c) Cross section, X 500.   L-65-7997

Figure 35.- Appearance of coating 11 on Cb-10Ti-5Zr alloy sheet in the as-coated condition.

59

Figure 36.- Mass change histories for specimens of coating 11 on Cb-10Ti-5Zr alloy sheet tested in air.
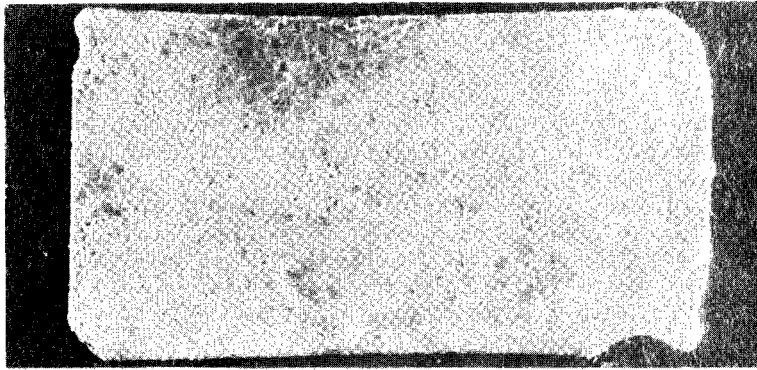
(a) 140-hour exposure at 2000° F (1365° K).
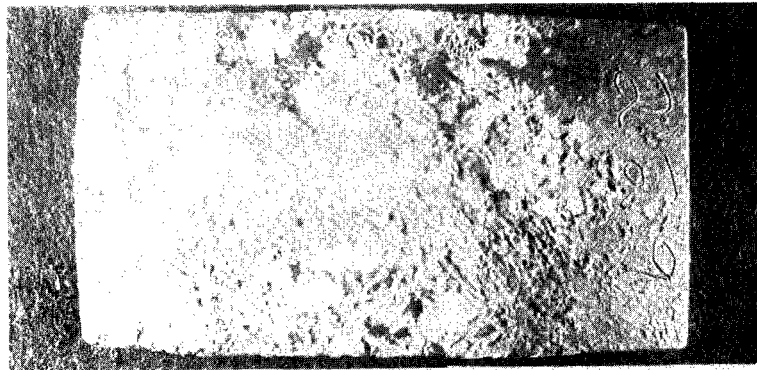

(b) 43-hour exposure at 2400° F (1590° K).

(c) 12-hour exposure at 2700° F (1755° K).   L-65-7998

Figure 37.- Photographs of tested specimens of coating 11 on Cb-10Ti-5Zr alloy sheet exposed in dry air at atmospheric pressure. X 2.

(a) 0.5 mm Hg $(66.7 \ N/m^2)$.


(b) 0.05 mm Hg $(6.67 \ N/m^2)$.   L-65-7999

Figure 38.- Appearance of tested specimens of coating 11 on Cb-10Ti-5Zr alloy sheet exposed for 20 one-hour cycles at 2400° F (1590° K) at reduced pressures. X 2.

(a) As-coated appearance, X 2.

(b) Cross section, X 100.
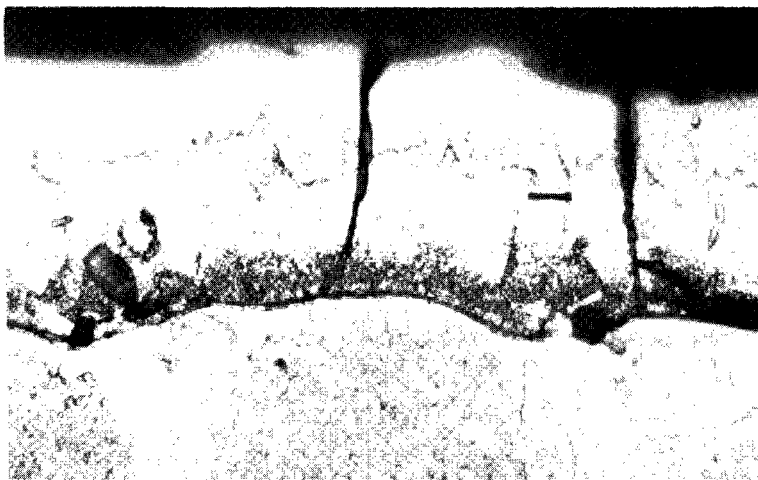
(c) Cross section, X 500.   L-65-8000

Figure 39.- Appearance of coating 12 on Cb-10Ti-5Zr alloy sheet in the as-coated condition.

Figure 40.- Mass change histories for specimens of coating 12 on Cb-10Ti-5Zr alloy sheet tested in air.

(a) 250-hour exposure at 2000° F (1365° K).
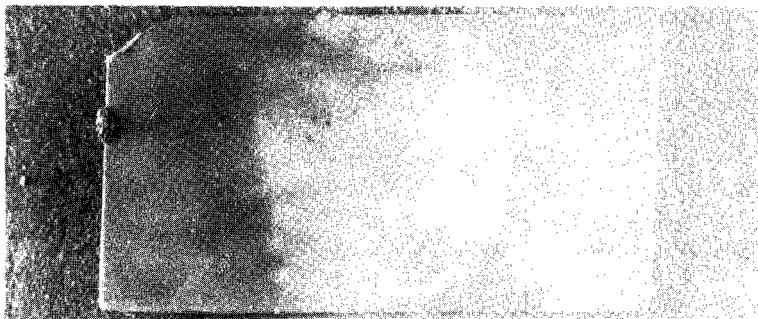
(b) 155-hour exposure at 2400° F (1590° K).
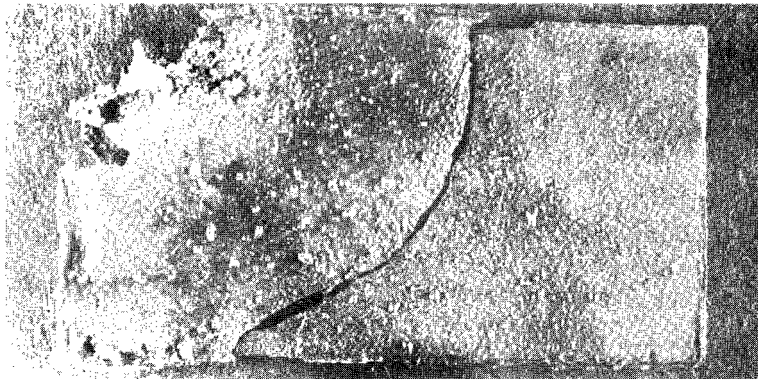
(c) 28-hour exposure at 2700° F (1755° K).   L-65-9001

Figure 41.- Photographs of tested specimens of coating 12 on Cb-10Ti-5Zr alloy sheet exposed in air at atmospheric pressure. X 2.
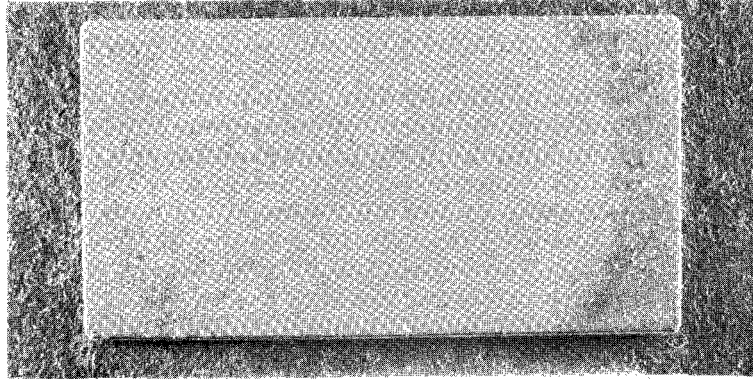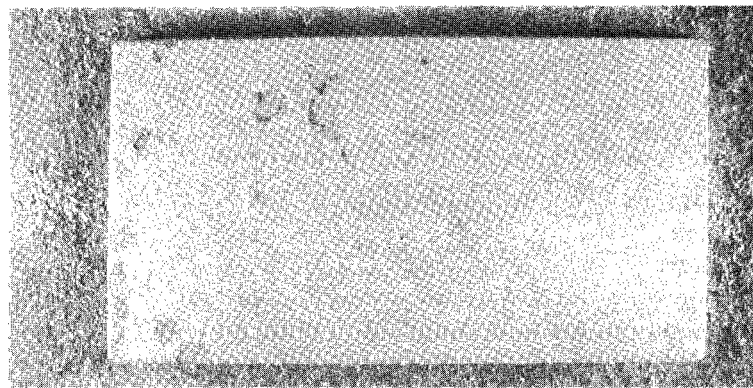
(a) 0.5 mm Hg $(66.7 \text{ N}/\text{m}^2)$.

(b) 0.05 mm Hg $(6.67 \text{ N}/\text{m}^2)$.   L-65-9002

Figure 42.- Appearance of tested specimens of coating 12 on Cb-10Ti-5Zr alloy sheet exposed for 20 one-hour cycles at 2400° F (1590° K) in air at reduced pressures. X 2.

Silicide coating

Cb—10Ti—5Zr alloy substrate (embrittled)

Conventional reflected light photomicrograph
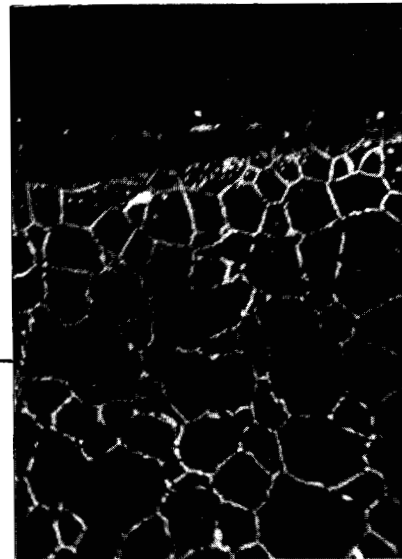
Photomicrograph by light of grain boundary fluorescence under electron beam.

Figure 43.- Photomicrographs of coating 6 on Cb-10Ti-5Zr alloy sheet in the as-coated condition. X 150.   L-65-9003

67
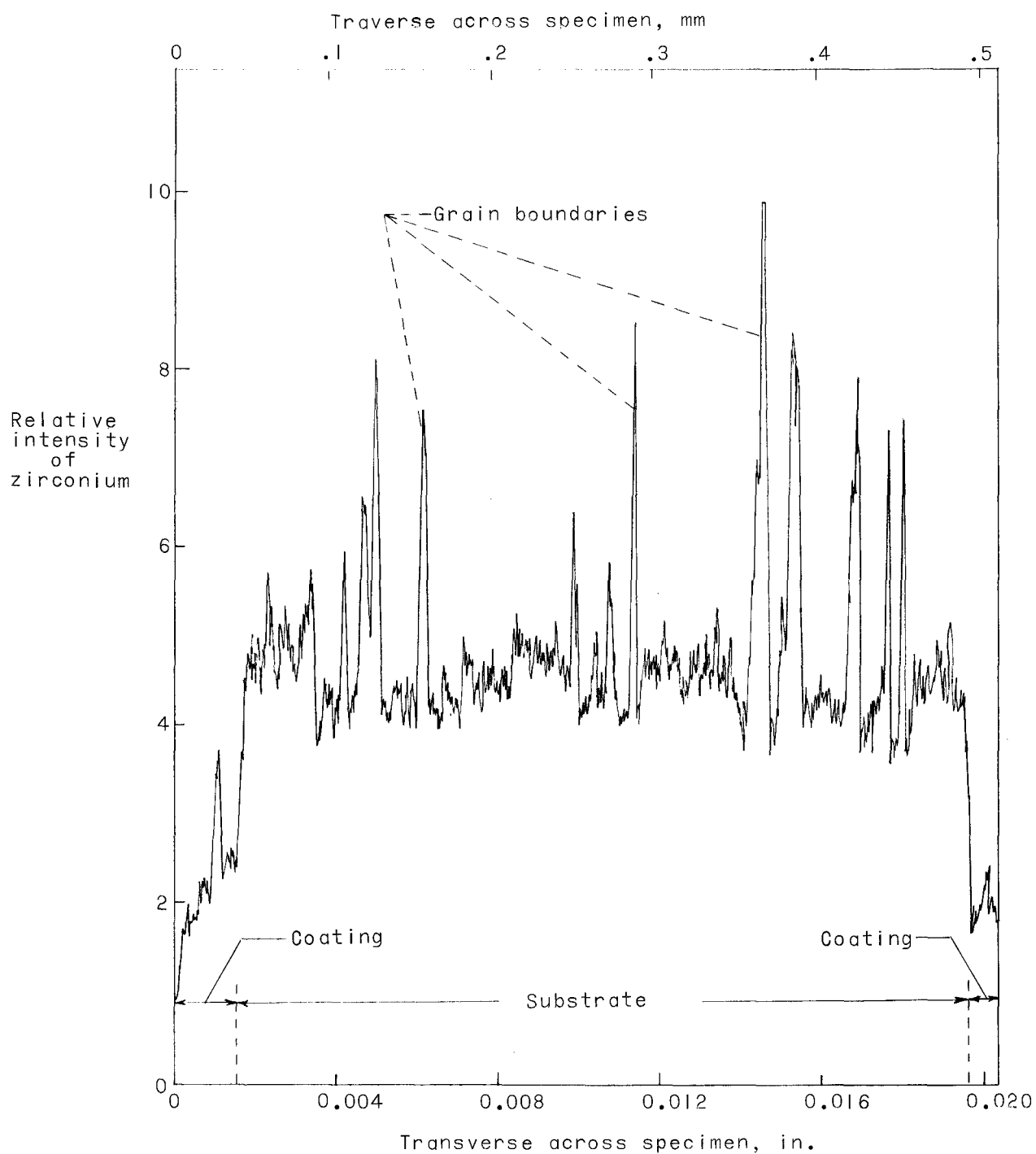
Figure 44.- Electron probe spectrographic traverse for zirconium across a specimen of coating 6 in the as-received condition.
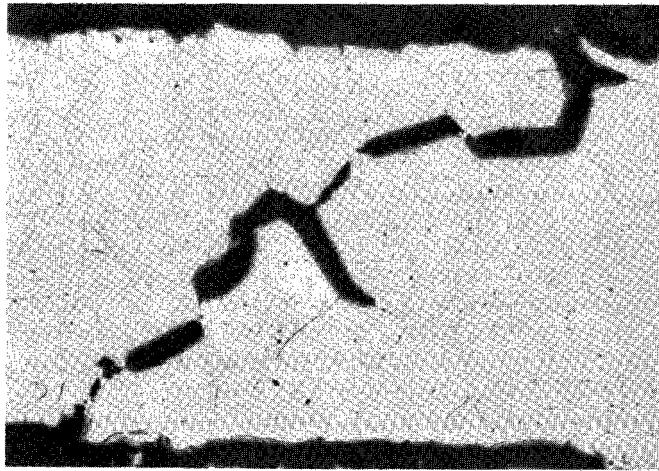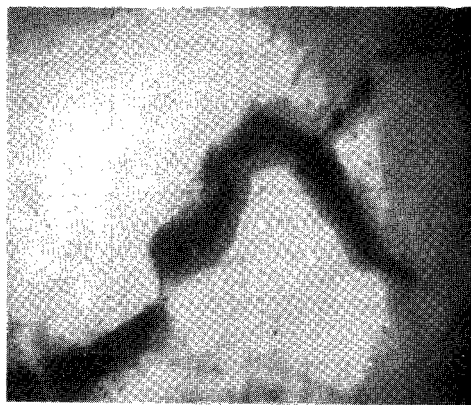
68
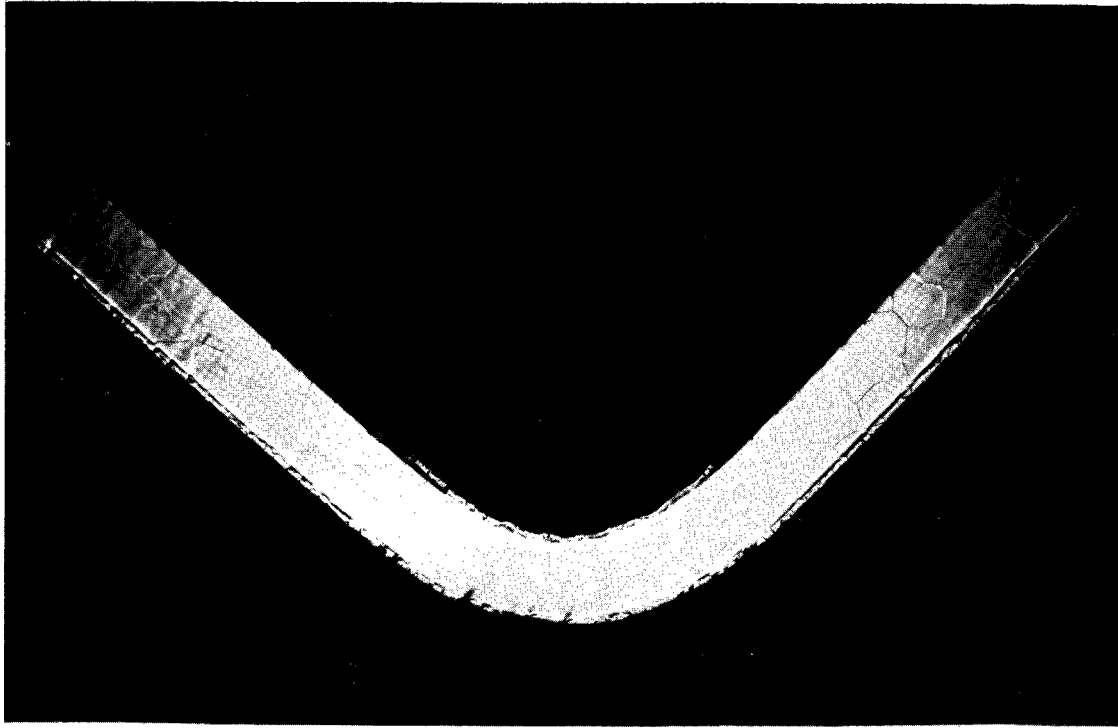
Figure 45.- Cross-sectional view of a specimen of coating 12 exhibiting a ductile bend after 240 hours   L-65-9004
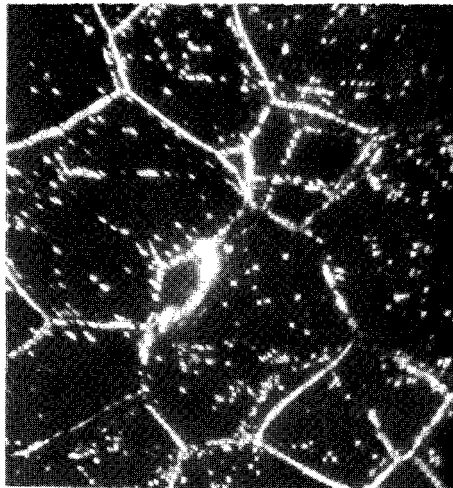of continuous exposure at 2000⁰ F (1365⁰ K). X 25.

(a) Bright-field illumination, metallograph, X 100.

(b) Bright-field illumination, electron
probe microanalyzer, X 150.

(c) Illumination by grain boundary
fluorescence under electron beam, X 150.   L-65-9005

Figure 46.- Cross sections of a specimen of coating 12, after 240 one-hour cycles at 2000° F (1365° K) in air
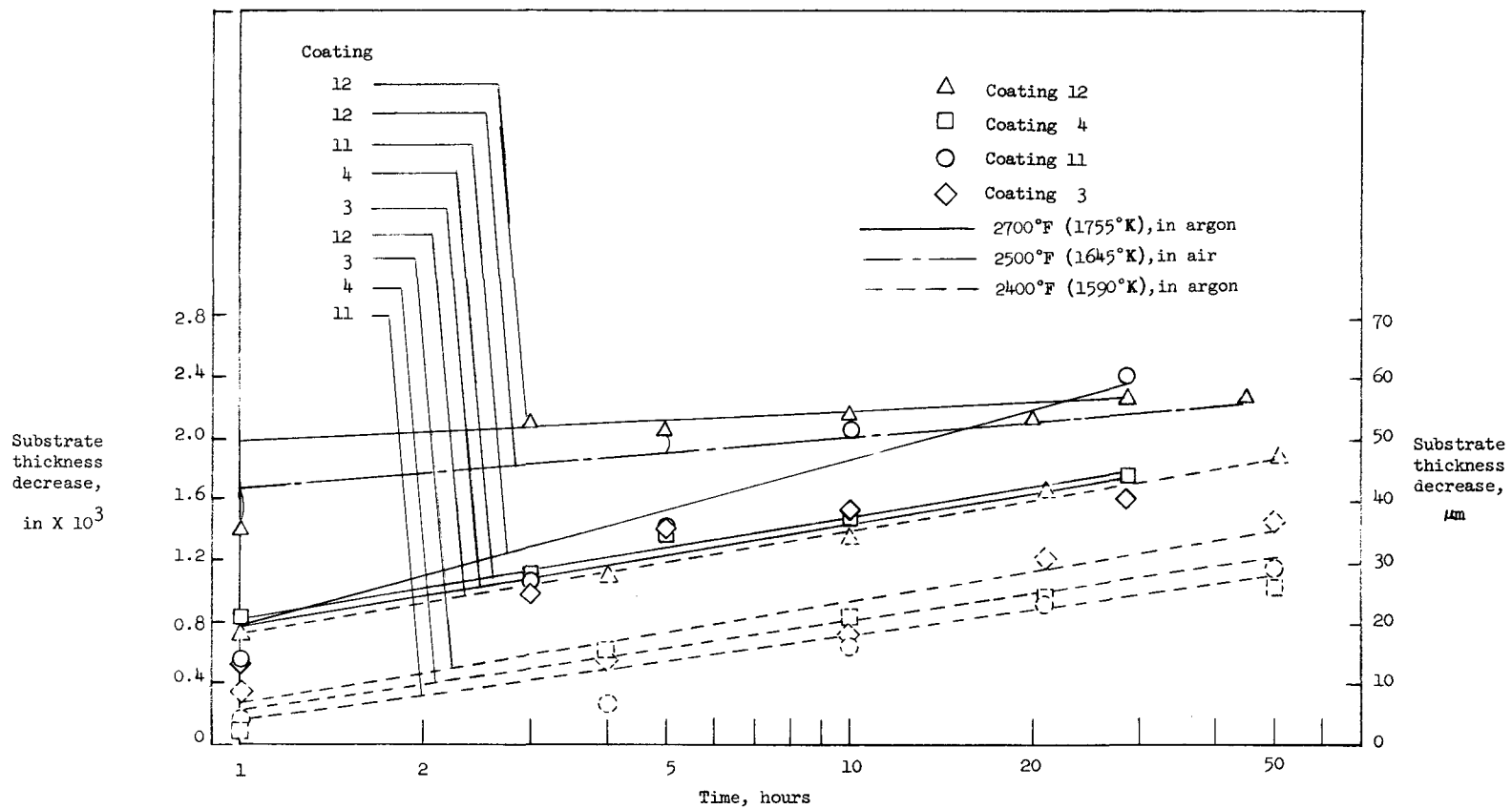at 760 mm Hg $\left(101 \text{ kN/m}^2\right)$ and a room-temperature bend test.

Figure 47.-   Substrate thickness decrease for several coatings on Cb-10Ti-5Zr alloy sheet at three temperatures.

NASA SCIENTIFIC AND TECHNICAL PUBLICATIONS

TECHNICAL REPORTS: Scientific and technical information considered important, complete, and a lasting contribution to existing knowledge.

TECHNICAL NOTES: Information less broad in scope but nevertheless of importance as a contribution to existing knowledge.

TECHNICAL MEMORANDUMS: Information receiving limited distribution because of preliminary data, security classification, or other reasons.

CONTRACTOR REPORTS: Technical information generated in connection with a NASA contract or grant and released under NASA auspices.

TECHNICAL TRANSLATIONS: Information published in a foreign language considered to merit NASA distribution in English.

TECHNICAL REPRINTS: Information derived from NASA activities and initially published in the form of journal articles.

SPECIAL PUBLICATIONS: Information derived from or of value to NASA activities but not necessarily reporting the results of individual NASA-programmed scientific efforts. Publications include conference proceedings, monographs, data compilations, handbooks, sourcebooks, and special bibliographies.

Details on the availability of these publications may be obtained from:

SCIENTIFIC AND TECHNICAL INFORMATION DIVISION

NATIONAL AERONAUTICS AND SPACE ADMINISTRATION

Washington, D.C. 20546